Modifying the Selectivity of Zwitterionic Copolymer Membranes by Molecular Imprinting

A thesis submitted by

William Lind

in partial fulfillment of the requirements for the degree of

Master of Science

in

Chemical Engineering

Tufts University

August 2016

Adviser: Prof. Ayse Asatekin

Abstract

Membranes are widely used to perform solution separations based on the size of solutes, but there are many applications where more complex basis of separation is needed. Molecular imprinting involves manufacturing a polymeric material (e.g. membrane or adsorbent) in the presence of a target solute that is later removed. This creates binding pockets that enhance the interaction of that solute with the polymer during operation, and can change the adsorption and permeation selectivity of the polymeric material. In this work, we utilize a molecular imprinting approach to combine the size-based separation capabilities of thin film composite membranes made from a zwitterion-containing amphiphilic copolymer with structure-specific separation capabilities. In so doing, we create a membrane that can distinguish between solutes based on size, but whose preference for selected solutes can be enhanced by simply altering the membrane manufacturing procedure. To achieve this, we prepared thin film composite membranes whose selective layers are formed by coating a thin selective layer of a zwitterionic copolymer blended with an imprinting molecule. We then characterized the performance of the membrane through filtration experiments. We saw that when a zwitterionic solute such as Vitamin B12 was used as the additive during manufacture, the permeation of that solute and other zwitterionic solutes was enhanced but that of other solutes (e.g. anionic dyes) was not affected. Interestingly, a similar effect was not observed when an anionic solute, Direct Red 80, was used for the imprinting step. This did not lead to any significant changes in membrane selectivity. Thus, based on our results to date, the molecular imprinting effect is specific to zwitterion imprinting agents and

solutes and is strongest when the imprinting agent is identical to the solute. Future work can better clarify what inter-molecular interactions lead to these results, and if the observed effect is general to all zwitterionic solutes.

Contents

Figures

Modifying the Selectivity of Zwitterionic Copolymer Membranes by Molecular Imprinting

1 Introduction

1.1 Overview

Liquid phase separation using membrane systems is gaining traction in industry because membranes are simple to operate, energy efficient, and can scale up easily on demand to meet process needs. Current membrane systems can separate components of feed streams by size, which is highly desirable in several applications including the removal of microorganisms from water both for drinking and biomedical use, removing organic macromolecules and oil from wastewater, concentrating proteins, and clarifying beverages [1]. Unfortunately, membranes today often cannot separate solutes of similar sizes, such as organic compounds or proteins in a mixture. This limits their applicability in many processes where thermal, extractive or chromatographic methods have to be used instead. However, because there are no commercially available membrane technologies which can perform separations based on size as well as structure of the solute, the ability to create such a system is a fascinating prospect and is explored in the following work.

The ability to separate components of a feed based on their size and chemical structure simultaneously would allow us to use a simple filtration unit operation for complex separations that would otherwise require methods such as extraction or chromatography. It could also condense multi-step processes that combine size-based and chemical structure-based separations to remove multiple types of contaminants into a single unit operation. This approach could replace the separation paradigms for the commodity molecule and drug industries. In a case like this, one membrane module could simultaneously separate large drug molecules from their synthesis side-products and

reduce the concentration of similarly-sized but chemically distinct analogs which may have no commercial utility.

In this project, we aim to address this need by modifying the selectivity of membranes developed in our research group through a process of molecular imprinting. Molecular imprinting is a process by which selectivity for a particular molecule or chemical class is induced in the adsorptive properties of a material [2]. This creates the ability to alter the selectivity of a membrane so that it may allow passage of similarly structured molecules which otherwise would not be separated effectively by the size-based separation capability of an untreated membrane. To create this preferential behavior, we manufacture custom membranes from solutions which contain the molecule we will subsequently be filtering. Having the so-called "target" molecule present when the membrane is being created, we impose sites within the membrane which are chemically complementary to the target and are capable of recognizing and allowing passage of similar molecules even after the target is removed.

In this work, we combine molecular imprinting technology with a novel approach for making membrane selective layers by polymer self-assembly. The proposed approach aims to expand the capabilities of novel membranes that are based on the microscale phase separation of hydrophobic and hydrophilic polymer segments, which have been shown to effectively and reproducibly yield membranes capable of separating solute molecules larger than 1 nanometer from those which are smaller [3]. The process of molecular imprinting has been deployed to create recognition sites in chemical sensors and adsorptive applications [4]–[6], but its introduction into steady-state filtration membranes for molecular separations is novel, with few previous studies [2], [7], [8].

The combination of self-assembly and molecular imprinting has the benefits of easy manufacture and controlled membrane selectivity that combines size-based and chemical structure-based mechanisms from a single operation. Specifically, we explore different film deposition and coating conditions to alter the selectivity of these membranes and to change the rejection of a particular solute or family of solutes without changing the effective pore size. Both polymer self-assembly and molecular imprinting occur spontaneously at the same stage in the manufacturing of filtration membranes. This means that there is effectively no additional manufacturing time needed to incorporate the chemical separation capabilities that arise from molecular imprinting in addition to the size-based capability of the self-assembled material. This ease of manufacture means that application of this technology could be cost effective while providing the ability to customize separations to fit the needs of any feed stream.

1.2 Membrane Separations and Design Criteria

Within the world of separation technologies, membranes offer several advantages over traditional techniques such as distillation, liquid-liquid extraction, and chromatography. Thus, membranes are gaining attention as a commercially viable process unit operation. Membranes do not require phase change of the separation media as in distillation, so energy usage can be cut dramatically [9], [10]. Additionally, there is no need to regenerate solid or liquid sorbents as in liquid-liquid extraction or chromatography, so membranes can be used as stand-alone unit operations. The nature of membrane-based separations means that a process can be scaled up or down simply by adding more (or removing) membrane modules, so a separation facility could easily change its scope in response to changes in demand.

Membranes are classified by the size of their pores, which determines the size of solutes or particles that will be retained, and therefore, the applications for which they are suited (Figure 1). Membranes are typically classified based on the separations they can perform and hence their effective pore size [1], [11], [12]. Membranes in the microfiltration (MF) category have pores which are on the order of 0.1 to 10 microns, making them useful for separating bacteria or particulates from a feed stream. Ultrafiltration (UF) membranes have slightly smaller pores, between 2 and 100 nanometers, and are typically tasked with separating proteins, viruses, and oil emulsions. The pore sizes for both of these types of membranes require that motion of solvent through them is accomplished by the pore-flow mechanism (see Section 1.3), and so the separations they perform are size-based [1], [13]. Nanofiltration (NF) membranes have an effective pore size in the range of about 1 to 10 nm and are used for water softening as they are able to filter divalent ions but have a low rejection of monovalent ions. To achieve total desalination of water streams, reverse osmosis (RO) membranes must be used. In this case, the membrane has a dense selective layer that no longer has channels of any discernable size. Transport through the materials in RO membranes is categorized as occurring by the solution-diffusion mechanism wherein separation occurs because of differences in the solubility and diffusivity of the various components of the polymer forming the thin selective layer of the membranes. Because nanofiltration membranes are used for solutes of size between those of ultrafiltration and microfiltration, the transport through these materials likely proceeds as a combination of the pore-flow and solution diffusion mechanisms [14]–[17].

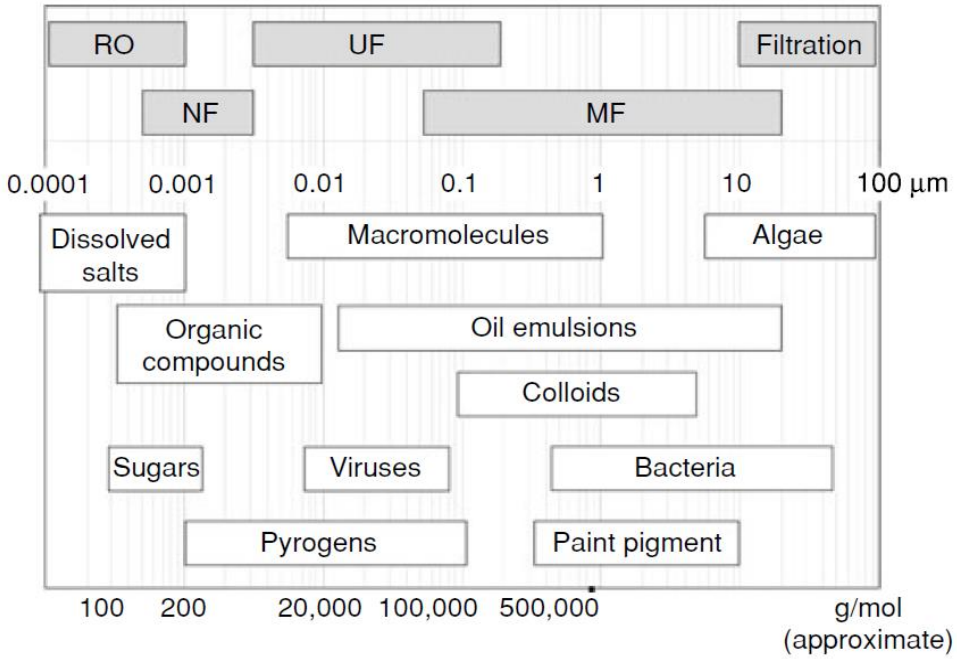

Figure 1: Relative size of solutes and the pore sizes of membranes capable of retaining them (Asatekin and Mayes 2009, Copyright ©2009 John Wiley & Sons, Inc. All rights reserved).

In general, separation technologies rely on selectivity to achieve their goal of yielding multiple streams with various compositions. For our purposes, the term selectivity refers to the ability of a membrane filtration system to separate molecules in a mixture by passing one through and retaining the other, and to do so with a high degree of preference. Typically, this means separating molecules of a particular size from those which are smaller. For good size-based separation capability, a membrane has to be able to do two things [12]: First, it needs to be able to accurately differentiate the size of molecules in a stream from molecules which are only slightly larger or smaller. Such a membrane allows for the separation of molecules which differ only very slightly in their diameter. Otherwise, it will only be applicable to separations where a very large solute is to be retained while very small solutes are to be allowed to pass through to the filtrate. Additionally, a separation unit operation should ideally fully retain large molecules while letting a very high proportion of small molecules through. In this case, there would be

very little leakage of large solutes through a membrane, and there would be very little resistance to the passage of small solutes. The most industrially relevant separations seek membrane selectivity that has both of these features so that solutes which are only slightly larger than the effective pore size are almost fully retained, while marginally smaller solutes are able to pass through unperturbed. This would allow the separated streams to have high concentrations of either small or large solutes without contamination of solutes which ideally would be relegated to another stream.

In addition to selectivity, an important design feature of a membrane system is the speed with which it is able to carry out a separation, quantified by the throughput of filtrate. The throughput of a membrane is reported as flux or permeability, depending on what information is required on the membrane. Flux is the volumetric flowrate which is achieved through a membrane module normalized by the surface area of the membrane:

$$J = \frac{Q}{A}$$

Where J is the flux [L/m^2.h], Q is the volumetric flow rate [L/h] and A is the cross-sectional area of the membrane [m^2] [1], [11]. Because membranes are often operated at elevated pressure to force permeant through more quickly, it is also useful to speak of the membrane's permeability which is the aforementioned flux further normalized to take into account the pressure difference between the permeate and retentate sides of the membrane:

$$L_p = \frac{J}{\Delta P}$$

Where L_p is the permeability [L/m^2.h.bar], J is the flux as discussed previously, and ΔP is the pressure differential across the thickness of the membrane. Membrane

permeability can be improved by optimizing certain parameters of the polymer morphology. When filtrate will be forced to travel through pores or channels in the material, flux will be higher in systems which have straight channels with low tortuosity. Low tortuosity membranes, therefore, allow the filtrate to cover the smallest distance necessary when traversing from one side of the membrane layer to the other. If the separation operation is achieved using a selective layer, as in our case, the flux will be higher if the composite membrane can be manufactured with the thinnest possible selective layer.

When designing a membrane material for separation applications, one must be especially conscious of the balance struck between permeability and selectivity typical of modern commercial membrane materials [10]. If a membrane contains a great many pores through its structure, it will tend to display a higher mass permeability. But if this larger porosity comes at the cost of a higher distribution in pore diameter, the size cutoff for solutes may be less defined [19]. Indeed, because of limitations in the modern membrane manufacturing process, most membranes with pores of uniform size contain fewer pores with further distances between them, leading to lower flux but with enhanced separation specificity. This is an important consideration because the use of a membrane with lower flux will require more modules to achieve a modest throughput, and will require more energy usage as they should be operated at a higher pressure to overcome their high resistance to mass transfer across their thickness. The necessity of this tradeoff in the modern membrane manufacturing techniques is one of the obstacles in the way of membrane separations that compete in scale with more conventional unit operations.

The performance of a membrane can be greatly hurt by a phenomenon known as fouling, wherein microorganisms, proteins or other feed components adsorb onto the membrane material and/or deposit on the membrane surface, thereby reducing its effective flux and separation abilities [1], [20]–[22]. This build-up of feed components at the membrane surface increases energy costs associated with the operation of the membrane, and significantly reduces its usable life.

To prevent, or at least limit fouling, two different approaches can be pursued. First, the hydrodynamics and operating conditions of the membrane module can be designed to minimize the accumulation of particulates on the membrane surface, and to prevent the formation of a thick boundary layer (also known as concentration polarization) that leads to an increased local concentration of foulants on the membrane [12], [20], [21], [23]. Second, the membrane materials themselves can be designed to minimize the adsorption of feed components on their surfaces [3], [21]. This must be tailored to the specific stream the membrane will be used to purify, as a membrane which is fouling resistant to one type of biomolecule may not work as well for another, and may have reduced efficacy [19].

In this project, we rely on the fouling resistant properties of zwitterionic materials. The density of charged species in zwitterionic materials leads to a high degree of hydration which greatly reduces the ability of proteins and other foulants to adsorb on these surfaces [24], [25]. This enables the membranes proposed in this study to be highly resistant to fouling by a wide range of organic compounds such as proteins and oils [3].

Depending on the materials employed and the manufacturing techniques, synthetic membranes can take on a number of different morphologies, as shown in Figure

2 [1]. If membranes are dense polymer films with no discernable pores, permeants will only be able to traverse the membrane by diffusion down a gradient of pressure, concentration or chemical potential. On the other hand, porous membranes contain voids in their structure. If the pores are of the same size throughout the membrane, it is said to be isotropic. Isotropic membranes separate permeants based on the ability of such molecules to pass through the voids to end up on the other side of the barrier. Anisotropic membranes are ones which have a distribution of pore size throughout the cross-section of the membrane. In order to increase the mechanical strength of a membrane, small pores can be created on the top of a material while the same material is used below as a porous support. In this case, the porous underlayer will not aid in the separation process but will hold in place and mechanically support the more selective top layer. Another morphology choice and the one used to create the membranes in this report, is the thin-film composite (TFC) asymmetric membrane. This morphology consists of a microporous support material onto which a more selective material is coated. This allows the selective layer on top to perform the separation while mechanical strength is conferred to the membrane by the thick porous material underneath. This decouples the material choice for the selective layer and the support layer, providing more degrees of freedom in membrane design [1], [12].

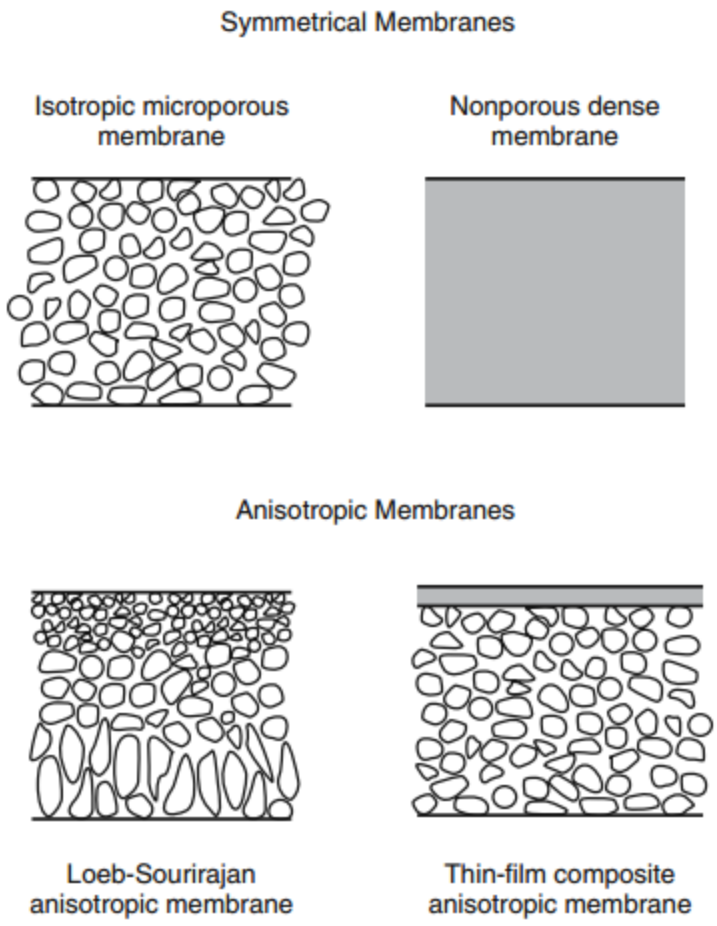

Figure 2: Schematic representations of various membrane morphologies in cross-section (Baker 2012, used with permission).

In this work, we chose to focus on TFC membranes that feature a thin, dense selective layer of a self-assembling polymer, applied by coating on a porous support. This morphology is similar to that found in commercial reverse osmosis and nanofiltration membranes. This project focuses on using different film deposition and coating conditions to alter the selectivity of these membranes, and to change the rejection of a particular solute or family of solutes without changing the effective pore size.

1.3 Transport Phenomena

While this thesis does not attempt to model transport through the produced membranes, in general, transport through media is modeled based on the morphology of the membrane or selective layer. In the case of a membrane with a dense, non-porous selective layer, the solution-diffusion model is used to describe permeation. If the driving force for diffusion arises from a concentration difference, the solution-diffusion model describes where the flux of solute between the upstream and downstream sides of the membrane as

$$J_i = -S_i D_i \frac{dc_i}{dx}$$

Where J is the flux, S is the solubility, D is the diffusivity, and the derivative is the change in concentration between the feed liquid and the permeate liquid. The driving force is ($\frac{dc_i}{dx}$), a spatial derivative over the bounds of the inner edges of the membrane medium. To permeate through in the absence of pores, the solute needs to partition into the membrane selective layer at the feed-membrane interface. The equilibrium constant of the solute between the polymeric selective layer and the solution, S_i, describes this step. This parameter may be thought of as the solubility of the solute within the membrane. The rate of transport across a membrane is also dependent on the diffusivity (D_i) which is unique to the solute-solvent system in question. The product of the solubility and diffusivity terms, $S_i.D_i$, is a measure of the permeability of the selective layer to the solute [1].

The diffusion coefficient can be derived kinetically for simplified cases involving liquid mixtures, and is a function of the effective cross-section of the solute and solvent,

their molecular weights and the number of molecules per unit volume for each species [26]. In this model, permeants are allowed to move through a medium (such as polymer scaffolding) because of openings between chains caused by random thermal fluctuations. With small enough solute molecules, their motion will be step-wise as the solute jumps from one microcavity to another, leading to macroscale smooth diffusion based on a concentration gradient.

On the other hand, if the membrane has discrete pores that allow permeation, the pore-flow model is in effect [1], [27]. In the case of a pressure driving force, this model is written mathematically as Darcy's law, which states that the flux of species *i* is a function of a scaling factor and the pressure gradient in space taken between both sides of the inside of the membrane material:

$$J_i = K' c_i \frac{dp}{dx}$$

Where K' is the hydraulic conductivity, a measure for how quickly a laminar flow can transport a liquid through a confined channel, c is the concentration of species *i* in the liquid and $\frac{dp}{dx}$ is the driving force for flow, in this case a pressure differential across the thickness of the membrane.

The solution-diffusion model typically dominates in membranes where the selective layer has no discrete pores, such as RO and gas separation. Pore flow, which leads to size-based separation, is dominant in porous membranes. In the systems proposed here, the estimated pore size is around 1 nm. While the data to date indicate a size-based separation scheme in agreement with a pore flow system, we would expect that in such a microphase-separated system, intermediate behavior that combines these

models may be in effect [28]–[31]. So, a combination of these models is likely necessary to describe flow through zwitterionic membranes because the materials used here are not wholly independent from the solutes and solvents being passed through them; some interaction is possible.

An important phenomenon to consider when studying the transport phenomena present during most practical applications of these membranes is that of concentration polarization. When membrane systems are used to separate a mixture, one species will be allowed through the membrane (i.e. the solvent) while another is retained upstream of the membrane (our large solutes), leading to a layer at the membrane surface that is enriched in the solute molecules and depleted in solvent [1], [20], [21]. When this happens, the ability of the membrane to separate effectively drops as the barrier interface encounters a solution of much higher concentration than previously. The higher solute concentration at the interface also increases the likelihood of fouling, where solute molecules adsorb onto the membrane surface and prevent the free flow of solvent through the pores of the material. To combat this, all of our experiments were conducted in stirred cells to reduce the boundary layer thickness and the effect of concentration polarization on the performance of our membranes.

1.4 Manufacturing Membranes by Immersion Precipitation

To create membranes from our polymer material, we require a technique for depositing a thin layer of polymer and hardening the polymer in place with a specified morphology. For this purpose, we will dissolve the polymer in a solvent, deposit a thin layer of this solution on a porous support membrane, and then remove the solvent. A simple method for this is to evaporate the solvent. Alternatively, we can use the method

of non-solvent induced phase separation (NIPS), also termed immersion precipitation, a membrane manufacturing technique developed by Loeb and Sourirajan in the 1960s [1], [32]. This method relies on the use of a polymer dissolved in a solvent, and a liquid which is miscible with the solvent but is known to precipitate the polymer referred to as the non-solvent. The polymer solution is spread either into a film on a non-stick surface (e.g. glass), or in our case, on a porous support, and then immersed into a bath of the non-solvent. The polymer coating will be hardened when the solvent is transferred into the non-solvent [9]. When the solvent is removed from the polymer (either by evaporation or incursion of non-solvent), a concentration gradient beginning at the surface of the coating forms, and the higher immediate concentration difference causes the material to undergo demixing and solidification into its final morphology [9], [33].

This approach can be used to produce a wide range of polymer film morphologies, from porous membranes with symmetric or asymmetric cross-sections (e.g. microfiltration and ultrafiltration membranes) to thin, dense membrane selective layers. If this phase separation occurs quickly, porous morphology can be expected in the solidified polymer layer due to transport limitations. The morphology of the polymer layer depends on both the solubility of the polymer in the solvent and non-solvent, and the relative diffusivities of the solvent and non-solvent. If the polymer has very low solubility in any solvent/non-solvent mixture, or if the solvent has a very high diffusivity in the non-solvent and vice versa, phase separation will occur very quickly. On a ternary phase diagram (such as Figure 3), this situation will be characterized by the polymer immediately crashing out of solution as the composition of the polymer layer plunges quickly into the spinodal region. This typically results in a porous membrane with an asymmetric cross-

section, featuring a thin layer on top with very small pores supported by increasingly larger pores. Such membranes are commonly used for ultrafiltration and microfiltration.

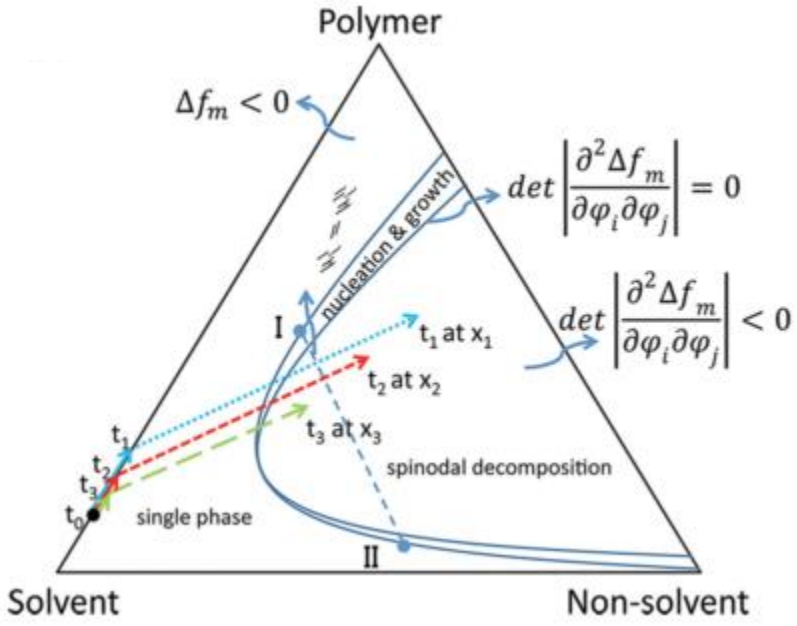

Figure 3: Ternary diagram of a polymer-solvent-nonsolvent system (Abetz 2015, used with permission).

If we instead want to form a thin, dense polymer layer by solvent inversion, we should select a non-solvent such that precipitation will be slow, and we enter the two-phase region gently (i.e. through the metastable or binodal region). In addition, it is crucial that the solvent's diffusivity into the non-solvent be higher than the non-solvent's diffusivity in the solvent. This results in the solvent leaving the polymer before the non-solvent enters the selective layer, and allows the collapse of the polymer layer into a dense film as opposed to a thick porous layer. Typically, if care is not taken with respect to one's location in the ternary diagram, membranes manufactured by phase separation tend to display higher porosity but lower selectivity than their counterparts made using other methods such as track etching [19], [34], [35].

The presence of additives in the coagulation bath can affect the membrane formation process [36], [37]. If some non-solvent is added to the casting solution dope, the solidification can happen faster, and more asymmetric porous membranes with thinner selective layers can be expected. Because we are attempting to alter the selectivity of membranes using additives, we must be cognizant of this potential so that we do not alter the morphology in trying to change the selectivity. In gas separation membranes, Aroon et al. (2010) even observed a change in small molecule selectivity with various additives to the coagulation bath and dope. Selectivity increased as these investigators moved the binodal region closer to the dope position on the ternary diagram. Morphology ultimately comes down to the specific solvent-nonsolvent miscibility and speed of demixing achieved upon solidification, so the selection of liquids to use in this process is of critical import.

Ultimately, there are many factors influencing the morphology of membranes produced by phase inversion. We must take great care to control the factors we can while observing those we cannot give a full understanding of the mechanism at play. The ultimate morphology can be dependent upon many factors, including the casting solution concentration and viscosity, polymer molecular weight, rate of solvent evaporation and duration of evaporation prior to precipitation, presence of additives in the casting solution, casting solution and precipitant temperature, and the humidity of the atmosphere in which the precipitation is taking place, to name a few [33].

1.5 Principles of Self-Assembly

In selecting materials and manufacturing techniques for the creation of our membranes, it is especially important that we use a system which can impart the

necessary structures for selectivity relatively easily. This can reduce the effort which must be put in by an investigator, lowering the potential for human error. To create systems which have size-based selectivity without great effort on the part of the manufacturer, we rely on materials with the ability to self-assemble. Self-assembly is the process by which materials find their most energetically stable configuration through random motion and stay in this configuration because of the potential well into which they have fallen. In the context of membrane materials, this often means that polymer chains will be allowed to move freely, but will be solidified in such a way that their final orientation is not random, but rather is representative of the most stable configuration [19], [33], [38]. Membranes can be made with regular repeating structures by incorporating segments of the polymer chain which are highly incompatible, but are covalently bonded. This incompatibility can take the form of very different chemical structures and is quantified by the Flory-Huggins interaction parameter, χ [33], [38]. In such a system, self-assembly would occur as the incompatible segments attempt to lower their interfacial energy while being constrained by their chemical bonds to one another. The balance between these competing forces causes microphase separation which, when solidified, creates nanometer-scale domains with properties specific to the material in those phases. Unless there is a large change in the chemistry or environment of the material, self-assembly will occur the same way each time polymer chains of the same material are set in motion, meaning that self-assembly is a good way to ensure repeatability of the structure with a narrow pore size distribution.

Nanoporous materials manufactured by self-assembly are gaining prominence because of the tools this process gives to researchers to influence the assembly to fit their needs [19]. Once made, membranes made by self-assembly can show high throughput,

high surface area and a homogeneity of pore sizes because of the ease with which highly regular repeating structures can be created [19], [39], [40]. This regularity of structure can be invaluable in applications where selectivity must be controlled precisely, and the ease with which self-assembly allows for this regularity make it extremely useful. For example, the self-assembly of block copolymers into pores during membrane formation can lead to membranes with high flux and very evenly sized pores. These membranes show promise in the purification of pharmaceutical products where viral particles must be controlled so as to release no more than a single retrovirus particle per million doses of drug produced [19], [41], [42].

Nanoscale structures are difficult to achieve without self-assembly as this process allows for rapid ordering based only on thermodynamic principles such as those predicted by the Flory-Huggins theory, and which proceed spontaneously in an appropriate environment [13], [19], [33], [34]. Self-assembly of block copolymers, whose chains consist of two segments or blocks of different monomers attached by a covalent bond, has been extensively studied and applied to membrane manufacture [19], [33], [34], [43]. In the case of block copolymer self-assembly, many uniform pores form when well-tuned processing parameters are used. Even when the polydispersity of the polymer is fairly high, the ordered structures assemble in the same fashion, indicating that the morphology of assembly is based on interactions between various parts of the polymer, and can typically be correlated with the radius of gyration [19]. This means, however, that creating pores outside the 10-100 nm range is quite difficult. The smallest domain size reported for a block copolymer is 3 nm [44].

For self-assembly to occur at smaller size scales, the correct copolymer architecture must be selected (typically comb-shaped [35], [40] or random [3]) and the

two types of repeat units must be highly incompatible [33]. This is why there are few reports of polymers that self-assemble in the 1 nm size range. For instance, poly(vinylidene fluoride)-*graft*-poly(oxyethylene methacrylate) (PVDF-*g*-POEM) has been observed to form bicontinuous nanodomains with semi-crystalline PVDF and POEM [35]. As a membrane selective layer, the POEM domains in this copolymer act as permeable "nanochannels" with an effective pore size of about 1 nm. When this material was deposited on a PVDF base membrane to form a TFC membrane, it exhibited a permeability of almost 9 $L/m^2.h.bar$, and it was capable of filtering dye molecules with enough specificity to distinguish between Congo Red (hydrodynamic diameter 10.05 Å) and Brilliant Blue (diameter 11 Å).

Recently, the Asatekin group has published work detailing how self-assembly of statistical copolymers can be used to create fouling resistant thin-film composite membranes which display size-based separation of solutes in the range of 1 nm [3]. The membranes used in this study are made from a copolymer of the hydrophobic monomer 2,2,2-trifluoroethyl methacrylate (TFEMA), and a hydrophilic zwitterionic monomer such as sulfobetaine methacrylate (SBMA). It is assumed that *Poly*(TFEMA-*random*-SBMA) (PTFEMA-*r*-SBMA) self-assembles into ~1 nm water-permeable nanochannels of zwitterionic groups, held in place by the hydrophobic domains.

PTFEMA-*r*-SBMA copolymers that contain approximately 40 wt.% SBMA were selected for this project because of their favorable fouling-resistance, filtration characteristics, and stability in saline solutions [3]. To prepare the TFC membranes, the copolymer is dissolved in a solvent and coated onto a porous support. It is then immersed into first isopropanol and then water to remove the solvent. Isopropanol enables the formation of a porous selective later due to its low diffusivity. The copolymer self-

assembles as it precipitates out of solution. The hydrophilic monomers will tend to aggregate together to maximize their interfacial contact with the water while the hydrophobic polymer sections will segregate into separate domains so as to limit their exposure to the water and the hydrophilic polymer pendant groups [3], [13], [19], [45]. Figure 4 shows a schematic representation of the self-assembled nanostructure.

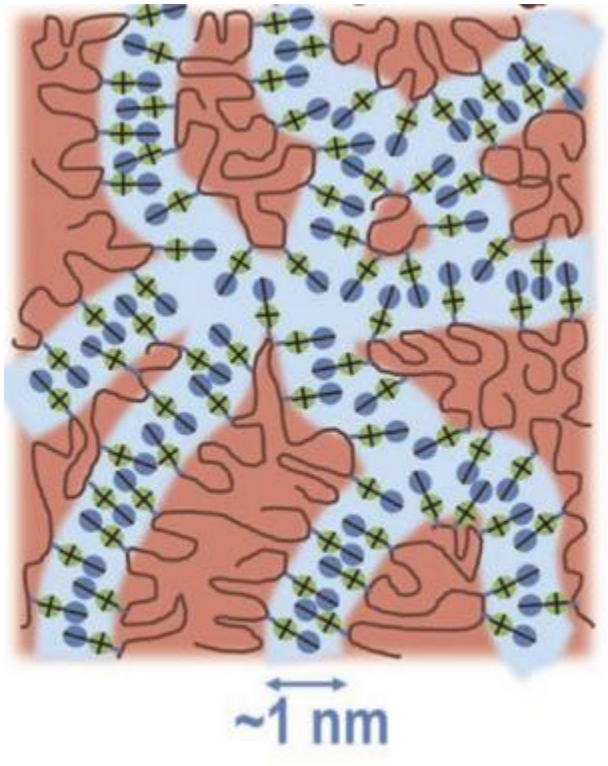

Figure 4: Proposed self-assembled nanostructure of the TFEMA-SBMA copolymer. Pink domains represent hydrophobic TFEMA, while blue channels represent hydrophilic SBMA.(Bengani et al. 2015, used with permission)

Previous studies using this copolymer system have led to the conclusion that the zwitterionic, hydrophilic segments of the polymer associate to form channels of zwitterion groups which fully penetrate a thin membrane coating [3]. It is believed that the SBMA pendant groups would self-assemble into an interdigitated arrangement, where the groups arrange in a “crisscross” pattern like folded fingers, aligning opposing charges [46]. This unique orientation creates a useful environment into which we can

tailor the interactions between the polymer and solutes. We propose to use the interdigitated domains as a platform to imbue the PTFEMA-*r*-SBMA copolymer system with selective interactions with specific solute types to create customizable filtration profiles based on how we allow these channels to self-assemble.

We believe that the interdigitation of the zwitterionic monomers in the self-assembled channels of our material plays a crucial role in the transport of solute molecules through these channels. While it is difficult to find past studies detailing the use of zwitterionic pendant groups in this type of morphology, there has been work done to elucidate the mechanisms at play in systems with nanochannels lined with functional groups generally. One study found that the addition of thiol groups to the inside of gold nanotubes could increase the hydrophobic preference of the material and that addition of pyridine increased the hydrophobic preference [47]. By increasing the size of the groups in the nanotubes, the researchers were able to increase the rate of permeation of specific solutes, depending on their chemical structure and their interaction with the functional groups on the channel walls. The inclusion of the functional groups onto channel walls decreases the effective size of the pore by occluding a portion of the free volume [46], however. While making the groups larger was found to decrease the diffusive coefficient in the tubes, it greatly increased the partition coefficient for the solute between the water and the membrane, thus increasing the overall rate of transport. [47]

1.6 Additives to Membrane Materials

This investigation focuses on finding ways to easily alter the selectivity of membranes without changing the polymer structure, so we turn to methods which are

easily tunable and can be implemented during manufacture without having to add many more steps to the process. The addition of small molecules into the casting solution has been suggested as a way to affect the orientation of polymer ultimately displayed upon solidification [9].

The use of additives in the polymer solution can create a casting environment which favors dense coatings as opposed to macrovoid-containing membranes [9]. This occurs by changing the phase diagram of the polymer solution/non-solvent pair. The most effective additives for controlling porosity are typically polymers with molecular weights on the order of tens to hundreds of kiloDaltons [9], [48]–[51], or simply solvents which can decrease the viscosity of a casting solution [52]–[54].

Beyond changing membrane morphology, additives can lead to changes in the molecular arrangement of the polymers forming a non-porous membrane selective layer, improving the balance between selectivity and flux. This is especially common in gas separation membranes that operate based on the solution-diffusion mechanism. For example, in the case of a poly(dimethyl siloxane)-*block*-poly(ethylene glycol) (PDMS-*b*-PEG) membrane proposed for use in CO_2 separation [55], polyether-*block*-amide was blended into the copolymer, yielding a membrane with enhanced CO_2 selectivity and increased permeation rate. It has also been found that addition of ethanol to the coagulation baths for certain gas separation membranes can serve to increase viscosity and chain entanglement by retarding the solvent inversion process [36], [56], [57].

This demonstrates the multitude of ways the addition of various polymeric and small-molecule additives to polymer systems can be used to alter membrane performance. In this work, however, we seek to alter membrane selectivity targeting the

separation of specific solutes by creating sites in the polymer which are complementary to the additive molecules we employ using a technique called molecular imprinting.

1.7 Principles of Molecular Imprinting

The concept of molecular imprinting in its modern sense was first proposed by Polyakov in 1931 and is beginning to see wider applicability in recent material studies [2], [58]. At its basis, molecular imprinting refers to a process by which a material such as a membrane or microparticle (either of which is referred to as the matrix material) is made complementary to a target or guest molecule so that future interactions between them are more favorable [2], [10], [58], [59]. Once this favorability is established, one type of molecule can be separated from a broad background of a myriad of other molecules with varying degrees of separation efficiency based on the relative affinity of each molecule contained in a series of solutes tested. Materials created this way have applicability in solid-phase extraction, chemical sensors (where imprinting can be used to induce selective binding to a transducer) [4] and artificial antibodies [2], [60], [61]. Within these applications, target molecules of the most interest are those which cannot easily be separated or recognized by conventional separation technologies, such as toxins, chiral drug molecules and complex biomolecules [6], [10], [58], [62]. Molecular imprinting as a technology has the benefits of tunable selectivity for a molecule (or class of materials which are chemically similar), physical robustness especially to thermal stimuli, and low cost of implementation [2], [63]. These positive qualities are seen especially when Molecularly Imprinted Membrane (MIM) materials are compared to their naturally occurring counterparts in the biological sphere, namely receptor binding of ligands and enzyme reactions [62], [63]. Some inefficiencies in these materials come from heterogeneity in the shape of the monomer-template complex and from binding site

inaccessibility which can result from excessive tortuosity in the case where sites are located within channels of the MIM [10], [64]. It can also take a significant amount of time to remove the guest molecule from the MIM; in one case a membrane imprinted with quercetin was observed to have leached only 2.3% of the template after 30 hours [65].

Because imprinting leads to increased adsorption, it might be concluded that this process will result in a higher rejection of imprinted solutes, as they will require longer to traverse the thickness of the membrane. This change would be modeled as a lower value of the diffusive coefficient, D in the solution diffusion equation discussed in Section 1.3. However, the process of imprinting also allows for higher partitioning into the membrane from the solution. This would represent a higher effective value of the S parameter in the solution-diffusion model. The competition of these forces ultimately leads to a lower rejection of solutes under the influence of selectively imprinted adsorption.

The process of imprinting can be modeled thermodynamically by realizing that for a molecule to create a site complementary to its shape, both the target and polymer must be partially immobilized, leading to an entropic and Gibbs free energy penalty which must be overcome [64]. The Gibbs free energy change upon immobilization takes the form

$$G_{bind} = G_{t+r} + G_r + G_h + G_{vib} + G_p + G_{conf} + G_{vdW}$$

which states that the free energy change upon binding (G_{bind}) of a template molecule to a matrix is equal to the sum of the energy change due to translational and rotational arrest (G_{t+r}), rotor freezing (G_r), hydrophobic interactions (G_h), soft vibration modes (G_{vib}), polar groups (G_p), conformational freezing (G_{conf}) and from van der Waals

penalties (G_{vdW}). As a result of this analysis, it can be intuited that more rigid structures have fewer solution conformations and are therefore better templates. Template affinity is enhanced by more functional groups which can find complementary sites in the matrix [64].

The complementarity upon which imprinting is predicated is achieved by introducing a small molecule in a way that allows the molecule to create sites of custom shape on the matrix material [2], [6], [8], [58], [60]–[62]. This can be done in the polymerization stage if appropriate, where cross-linkers create tight networks which form imprinted sites around the guest molecule. These sites will stay intact even after removal of the imprinting agent, leaving behind indicators of its shape and electronic structure. The technique has been applied with success to imprinted particles which can be assembled into membrane materials, but there is increasing interest in imprinting to conventional membrane materials directly [10], [60]. The mechanics of imprinting rely on the fact that the imprinting molecule can be removed from the larger material network without damaging the sites it has created. To this end, imprinting uses the formation of either reversible covalent bonds between the guest and the matrix (such as those between a metallic species and an organic one), or weaker interactions such as hydrogen bonds, ionic interactions, Van der Waals interactions or π-π electronic interactions [2], [4]. From a heuristic standpoint, if too small a proportion of guest molecule is used during imprinting, there are simply too few interactions for a meaningful number of active sites to be formed. Conversely, if too many guest molecules are used per volume of the matrix material, the sites may become non-specific, and selectivity for the guest molecule and materials like it drop. It is also difficult to achieve a good concentration of imprinted sites since they are randomly distributed [60]. This makes it difficult to achieve both good

separation and imprinting selectivity, leading to the development of Composite Imprinted Membranes (CIM) which has one layer devoted to size-based separation and another used for imprinted sites [10], [60]. Molecular imprinting has been applied with great success to separation systems based on adsorption [5], [6], but there is little evidence that it has been applied in conjunction with size-based separation in a single material. It is a combination of these types of functionality that we seek in this study by applying imprinting to a material which has already been shown to separate based on size.

In some cases, the molecule we would like to imprint is hazardous to use, or expensive. This may make it more feasible to use a so-called dummy molecule for the imprinting process [2]. To create imprinted sites which are transferable to the molecule of interest, the dummy molecule must have similar functional groups or be structurally analogous with similar spacing between functional groups. Because imprinting creates sites which are complementary to certain structural elements of a molecule, it is possible to create sites which are highly selective for one type of molecule but are also somewhat selective for molecules in the same chemical family. An example of the transferability of imprinting selectivity from the guest molecule to others which are structurally similar can be seen in a case where gold electrodes were imprinted with cholesterol in a matrix of hexadecyl mercaptan [63]. In this case, it was shown by changes in the electrical properties of the electrodes that the cholesterol binding sites were being filled and that performance leveled off when the sites reached full template re-adsorption. The change in electrode performance was not seen when the system was charged with molecules dissimilar in structure to cholesterol, and the change was observed at a lower magnitude for structural analogs cholic acid and deoxycholic acid.

This concept is of special importance in this investigation since we see evidence that by imprinting for one zwitterionic solute, we can create selective separation for other zwitterions, meaning that we may be able to achieve separations for multiple chemically-similar solutes by the incorporation of just one additive solute.

In the proposed work, various additive compounds were combined with our copolymer material to achieve this molecular imprinting effect, by altering the spatial arrangement of the zwitterionic groups forming the hydrophilic domains during the precipitation of the copolymer. The desired effect was that having these molecules present while channels were self-assembling would impose a complementary structure in the polymer chains until they were fixed in place by the solvent exchange procedure. Ideally, once the rigid walls were set by immersion in non-solvent, the additive could be washed away to leave only the copolymer in its modified self-assembled morphology. Therefore, an ideal additive/imprinting molecule is one that is insoluble in the isopropanol bath into which the copolymer membrane is initially submerged, keeping it in place as long as the polymer is semi-solvated. Once the copolymer has been washed in IPA, the additive molecule should be fixed in place while the membrane is transferred to the water bath for non-solvent hardening. In this step, the solvent is washed away and the membrane hardens into its final state. Therefore, the presence of the additive in the appropriate molecular location is critical at this point in the membrane manufacturing process. Once the copolymer is hardened, the additive should wash away by its solubility in water, and its weak (non-covalent) adhesion to the polymer structure. In selecting candidates for additive compounds, we seek a molecule that will form only physical attractions to the water-permeable microphase in our polymer structure. This is to ensure that an additive can be washed out of the membrane quickly. Additives are investigated

here with special interest because they allow for the selectivity of the membrane to be customized very easily. It may be the case that selectivity can be altered by changing the copolymer composition or by finding a new polymerization regimen, but we seek a facile method to create customized selectivity which can be employed in the step where the polymer is being cast into membranes, not when the polymer is being synthesized. By focusing on imposing our alteration at this point, we allow large batches of polymer synthesis to be carried out without having to create a new and expensive synthesis protocol for each alteration method we wish to implement and test.

1.8 Interactions of Zwittermaterials

The zwitterionic functional group of interest to this study, sulfobetaine, has been studied in molecular simulations where it was compared to other zwitterions in terms of hydration characteristics and dynamics [66], [67]. In a comparative study, sulfobetaine has been found to have a high association number with sodium ions, and association number is less affected by the size (Van der Waals radius) of a salt cation [67]. The results of simulation experiments conducted on various zwitterions also indicate that sulfobetaine has a higher degree of hydration around the anion portion of its structure [66], [67]. Sulfobetaine was found to have three coordination shells associated with its anion, leading to a much larger shell volume than other zwitterions [66]. Across the whole of the molecule, sulfobetaine has a total of 25 water molecules in its first hydration shell alone, leading to its strong anti-fouling properties and potential swelling ability.

The interactions of zwitterions with one another and with solutes are different from the interactions of typical ionic species. In polymeric materials that contain zwitterionic pendant groups, the pendants can associate “intra” where one zwitterion

folds in upon itself to form a ring (as displayed in Figure 5) [25]. In this formation, the positive and negative charges on one zwitterion collapse onto each other. These species can also associate “inter” wherein pendant zwitterions from different parts of the chain cancel their respective charges by forming a complex of two zwitterions. This type of association can occur through either formation of a head-to-tail complex or a dimer. Depending on the location of each zwitterion involved in an inter association, this can lead to a single polymer chain being folded on itself, or two chains being loosely bound to one another. Thus, zwitterions are especially capable of interacting with other zwitterionic species in spatially specific ways. While they interact with charged species well, these interactions are not necessarily as well-defined. We would, therefore, expect interactions between a zwitterion-containing copolymer and a zwitterionic guest molecule to be especially interesting for molecular imprinting purposes.

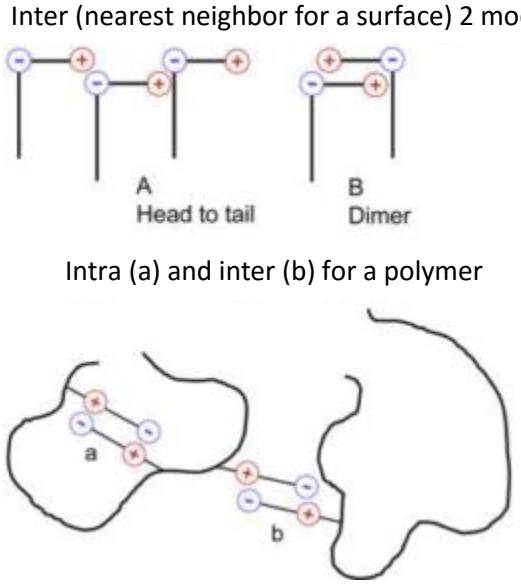

Figure 5: The various types of zwitterion interactions (Adapted from Schlenoff, 2014 used with permission).

1.9 Research Objectives

The investigation detailed herein aims to alter the selectivity of membranes whose selective layers are formed of the zwitterionic random amphiphilic copolymer PTFEMA-*r*-SBMA by using additives during membrane manufacture. Previous work on these membranes shows that they have ~1 nm pore size, high flux, and excellent fouling resistance [3]. Here, we explore manufacturing techniques and their effect on the pore size of the resulting membranes. Because of the broad range of solutes whose separation and purification could be of industrial significance, any customization of the filtration properties would be extremely important in the commercialization of this technology, especially if these changes could be accomplished by manufacturing steps instead of requiring a new chemical synthesis to be developed. We begin by investigating the possibility of shifting the pore size distribution to a larger effective diameter, ideally without sacrificing the narrow pore size distribution. Next, the concept of molecular imprinting is employed to probe whether it may be possible to leave the pore size unchanged, but to alter the way a particular solute interacts with the membrane material to create a different filtration profile for one molecule (or a class of molecules) within the group of solutes filtered. In each of these cases, we attempt to alter the filtration characteristics by the inclusion of small molecule solutes in the membrane casting solution. It is important for this investigation that any change that is achieved does not sacrifice the other properties of the membrane material, so special care is taken to measure and report thermal and morphological data to confirm that the additives used are not substantially altering the polymer's stability.

2 Experimental Methods

2.1 Materials

The zwitterionic monomer used in this study, sulfobetaine methacrylate (SBMA), along with the initiator azobisisobutyronitrile (AIBN), the inhibitor 4-methoxy phenol (MEHQ), the dissolution aid lithium chloride (LiCl) , Vitamin B12, Direct Red 80 and PPS were purchased from Sigma-Aldrich (St. Louis, MO). All were used as received. The glassy monomer used, 2,2,2 trifluoroethyl methacrylate (TFEMA) was purchased from Scientific Polymer Products (Ontario, NY) and was purified of inhibitor prior to use using an activated alumina column. Deuterated dimethyl sulphoxide (DMSO-d_6) for use as a solvent in NMR studies, was purchased from Cambridge Isotope Laboratory (Tewksbury, MA). The base membranes onto which our thin film was coated was a PVDF 400R ultrafiltration membrane obtained from Sepro Membranes (Oceanside, CA). The deionized water used for the experiments was generated by a building-wide Mar Cor Purification (Lowell, MA) unit. The isopropyl alcohol used as a polymer washing solution was purchased from Macron (Center Valley, PA).

2.2 Copolymer Synthesis

The PTFEMA-*r*-SBMA copolymer termed P40 throughout the rest of this document, was synthesized by the free radical copolymerization of 2,2,2-trifluoroethyl methacrylate (TFEMA) with sulfobetaine methacrylate (SBMA), as shown in Figure 6. First, 12g of SBMA monomer was dissolved in 320 mL of dimethyl sulfoxide (DMSO) along with 0.15g of lithium chloride to aid in monomer dissolution. TFEMA was purified to remove the inhibitor used in shipping by passing it through a basic activated alumina column. 18g of TFEMA was added to the reaction mixture. 0.032g of azobisisobutyronitrile (AIBN) was

added to the monomer solution as a thermal initiator. The reaction flask was sealed and heated to 70°C in a silicone oil bath. While the flask was reaching the initiation temperature, nitrogen gas was bubbled through the solution to remove oxygen for a minimum of 20 minutes. After at least 20 hours of reaction, the flask was removed from the oil bath and unsealed. 4-methoxyphenol was added as an inhibitor to terminate the free radicals and end the reaction. To purify the solution, it was precipitated in a ~2L bath of non-solvent made up of 50% ethanol in hexane. This non-solvent was swapped out every ~8 hours three times. The solid was vacuum filtered between each exchange. This non-solvent wash cleansed the polymer of the LiCl dissolution agent, as well as unreacted monomer and initiator. The polymer was then dried at 50°C in a vacuum oven.

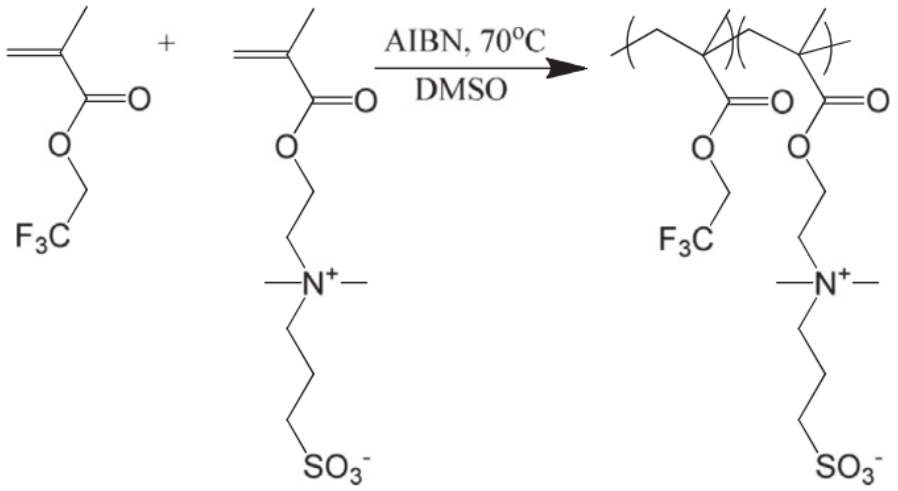

Figure 6: Synthesis reaction equation for P40 from its monomer constituents (Bengani, Kou, & Asatekin, 2015 used with permission).

Copolymer composition was determined using ^{1}H-NMR spectroscopy using a Bruker 500 MHz spectrometer (Bruker AVANCE III). To begin the sample preparation for spectroscopy, about 7.5 mg of lithium chloride was dissolved in 0.75 mL of DMSO-d_6 overnight. The next day, 4-5 mg of the copolymer was dissolved in the deuterated

solvent/salt solution. 128 scans were performed per test, with a D1 value of 10 seconds to allow adequate time for polymer relaxation.

Using the peak locations indicated in Figure 7, it is possible to calculate the relative molar ratios of each polymer pendant group. Subsequently, knowledge of the molar weights of each monomer allows conversion to weight percentages of each monomer in the final polymer structure. An example calculation of molar ratio is shown in the appendix.

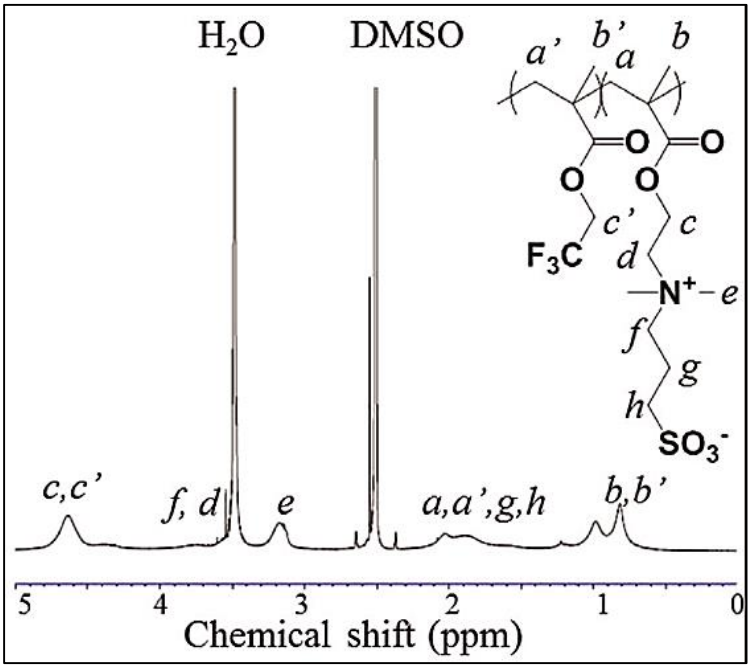

Figure 7: Typical 1H-NMR plot for the P40 material. Peak labels correspond to the portion of the chemical structure responsible for each peak (Bengani et al., 2015 used with permission).

2.3 Membrane Casting

Thin film composite (TFC) membranes with P40 selective layers were prepared using procedures modified from past publications [3]. P40 was dissolved into trifluoroethanol (TFE) at 50°C to create a 10% w/v solution. This polymer solution was filtered through a 1-micron glass fiber syringe filter (Pall Corporation, Port Washington,

NY) to remove impurities such as dust and undissolved clumps of the polymer. Because this syringe filtration creates bubbles in the solution, the solution was then degassed at 50°C for at least one hour. The filtered polymer solution was cast into a membrane by being spread onto a commercially available PVDF 400R ultrafiltration base membrane (Sepro membranes, Oceanside, CA) by a doctor blade (Universal blade applicator, Paul N. Gardner Company, Pompano Beach, FL) with an adjustable gate opening set to 25 microns. The coated polymer solution was immersed in a bath of isopropyl alcohol immediately after drawing with the doctor blade to slowly leach out the solvating TFE. After 20 minutes in the isopropanol bath, the membrane was moved into a DI water bath to solidify it in its final morphology. Initially, a series of experiments were conducted on membranes which were transferred to the IPA wash bath after being left in open air for various amounts of time. This allowed the TFE solvent the opportunity to evaporate off from the polymer solution, thus shrinking the thickness of the swollen polymer layer before it was solidified. In this case, the coated membranes were left to dry in a fume hood for a duration of 30 seconds, 2 minutes and 11 minutes. Membranes that were not part of this specific series were immersed into the isopropanol bath immediately after coating.

Membranes were also cast from the TFE solution phase onto base PVDF membranes and were immersed directly into water after the TFE was given time to evaporate into the air. This removed the TFE solvent from the polymer solution and shrank the swollen copolymer so that it would form a thin, dense coating when transferred into the water.

2.3.1 Morphological and Thickness Analysis by Scanning Electron Microscopy

In order to image the polymer selective layer achieved using the copolymer, a Phenom G2 Pure Tabletop Scanning Electron Microscope (SEM) operating at 5 kV was used to take cross-sectional images of the copolymer layer on the PVDF base. Coated membranes samples for imaging were taken from the same coated sheets used for filtration tests and were freeze-fractured in liquid nitrogen to cleanly expose the inner cross section of the material to the electron beam. Fractured samples were mounted on imaging stages and were sputter coated with gold-palladium to increase the electrical conductivity and the acuity of the microscope. Within the Phenom user interface, it was possible to measure the thickness of the polymer coatings observed. A sample image is shown in Figure 8.

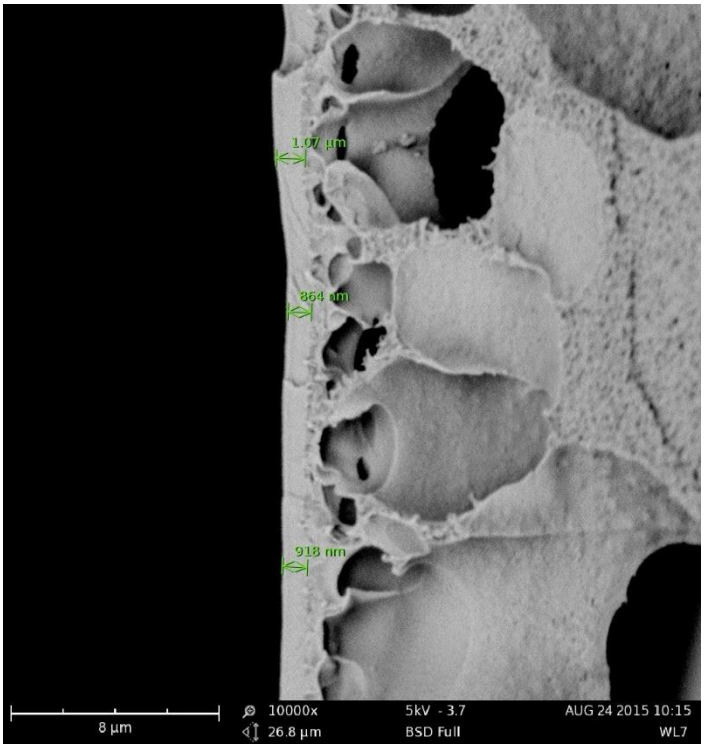

Figure 8: Scanning Electron Micrograph of a thin film composite membrane cast from P40 onto a PVDF base. Measurements were made through the Phenom microscope computer.

2.3.2 Aqueous Filtration Experiments

The performance of the prepared membranes was quantified by measuring water permeance and the rejection of several organic solutes in dead-end stirred cell filtration experiments using a set of Millipore Amicon dead-end filtration cells at one of two sizes: 10 mL volume with active surface area of 4.1 cm^2, or 50 mL volume with 13.4 cm^2 membrane area. The larger cell was used in cases when the flux through the membrane was too slow to allow tests to be conducted in a timely manner using the smaller surface area cells. The membranes were compacted and stabilized by filtering DI water through them at 30 psig. During the initial water compaction stage, the permeance of water was observed to begin at a high value and equilibrate to a lower value after about ninety minutes of compaction (Figure 9). Water was permeated at this higher pressure for an adequate amount of time so that the permeance leveled off at a stable value before actual dye filtrations were begun.

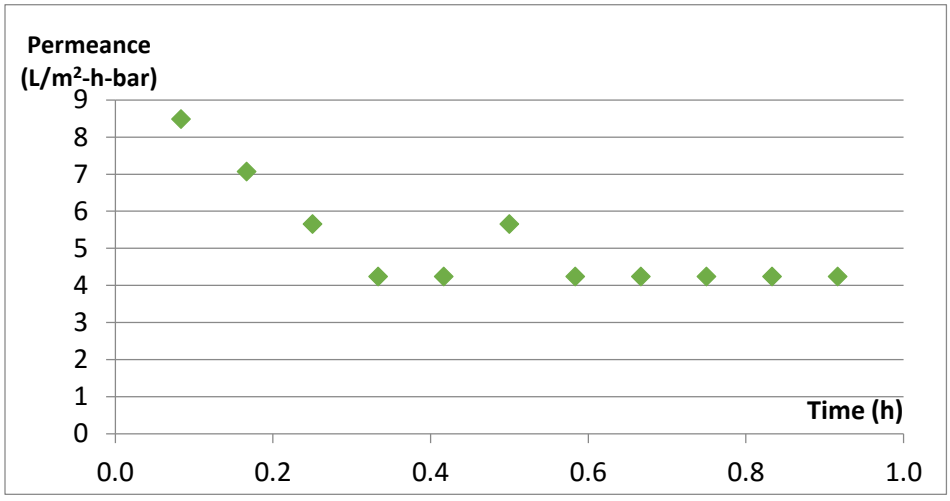

Figure 9: Typical high-pressure compact plot displaying the evolution of permeance over the time required to complete the initial compaction.

To characterize the effective pore size, or size cut-off, of these membranes, a series of organic solutes, typically organic dyes or vitamins, were filtered through the

membrane at 20 psig and their rejections were calculated. The computer package Molecular Modeling Pro (version 6.3.6) was employed to estimate the diameter of a range of organic molecules. This allowed for the creation of a set of dyes with which a rejection curve based on size could be constructed. This computer package uses atomic interaction equations including Lennard-Jones to manipulate a 3-dimensional model of a molecule until each atom has reached a stable configuration in space with respect to its neighbors. A list and the relative sizes of all solutes used in this study are given in Figure 10. It must be noted that the sizes calculated using the molecular volume of the molecule not taking into account any hydration shell. The diameter reported here is calculated from the molecular volume assuming each molecule is spherical, which may also skew the calculated size.

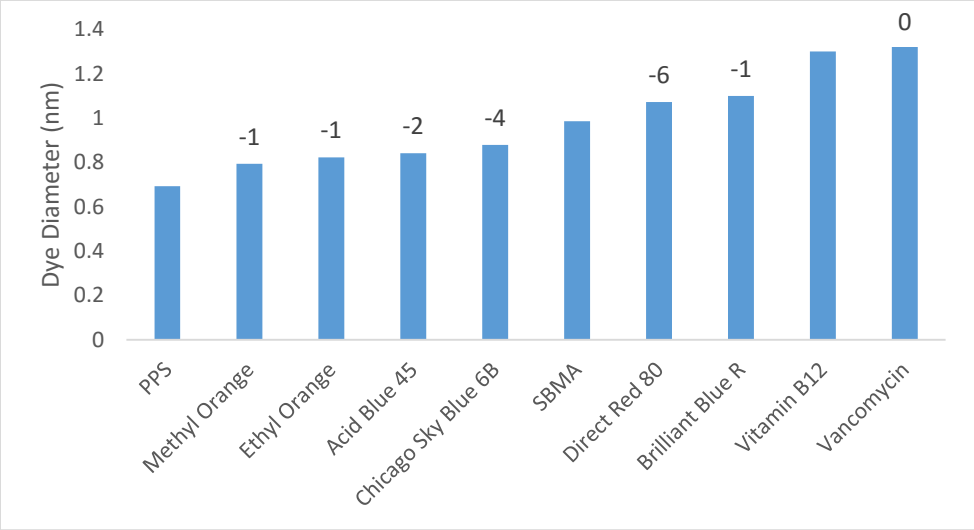

Figure 10: Size of feed dyes used in filtration experiments overlaid with molecular charge. Vitamin B12, SBMA, and PPS are not given a charge label as they are zwitterionic and therefore contains balanced charges.

To measure the rejection of each solute, a 100 ppm (w/v) solution in water was filtered through the membrane at 20 psig. When a dye was first charged to the membrane 1 ml of liquid (or about 1.7 mL, in the case of the larger cell) was permeated and discarded

before taking a sample, to account for the hold-up volume of the cell and allow stabilization. The next 1 mL of filtrate was collected in a clean glass vial which was resting on the weigh plate of a Scout Pro SP401 balance (Ohaus, Parsippany, NJ) connected via USB to a Dell laptop data collection station. Readings from the balance were logged by TWedge 2.4 software (TEC-IT, Austria) at a data collection rate of two readings per minute, which allowed calculation of the permeance.

The concentration of the solute in the feed solution (100 ppm) and filtrate were determined using UV-visible spectrometry in a Thermo Scientific Genesys 10S ultraviolet-visible spectrometer (Thermo Scientific, Waltham, MA). From these concentrations, the rejection was calculated according to:

$$\mathbb{R} = \left(1 - \frac{c_{jl}}{c_{j0}}\right) * 100\%$$

Where c_{jl} is the concentration of dye in the filtrate and c_{j0} is the concentration of dye in the feed. The calculated rejection of each dye was plotted against the size of the dye to create a rejection curve plot. Because of the accuracy of this instrument, it was important to ensure that all additives were washed out of the membranes before filtrate testing began. Though only a small amount of additive would be expected to wash out during dye tests, any amount of additive molecule in downstream filtrate samples could upset the ability of the UV/visible spectrometer to measure the filtrate concentration of the feed. For this reason, water was always filtered through the membrane devices before dye testing started to make sure they were free of solute.

2.3.3 Thermal Analysis

An important method for testing and characterizing the polymeric materials made for this study is Differential Scanning Calorimetry (DSC) which allows for probing of the thermal properties that exist at various temperatures along a spectrum. For these studies, a Thermal Advantage Instruments DSC Q100 V9.9 Build 303 unit was used in power-compensation mode to perform modulated temperature profile calorimetry experiments. Approximately 3.5 mg of the polymer sample was crimped into an aluminum pan, and the test chamber was flushed with a nitrogen gas flow at 50 mL/min. The temperature in the test chamber increased from -80^{o}C to 240^{o}C at a rate of 3°C/min and was modulated by 1.0°C every 40 seconds.

2.3.4 Nile Red Absorbance Tests

In order to test the potential segregation of Nile Red into the microphases of the copolymer as a representative additive, a number of polymer solutions with this dye and similar solutions without the dye were created to serve as standards against which the absorbance contribution of the dye could be clearly seen. The polymer solution reference standards were created using 4.5g of TFE to dissolve .5g either TFEMA homopolymer (solution A), SBMA homopolymer (solution B) or P40 copolymer (solution C). Similar polymer solutions were made along with 0.0125g of Nile Red dye. The TFEMA solution containing Nile Red was labeled solution D, while the SBMA solution with Nile Red was labeled solution E and the P40 solution with Nile Red was labeled as solution F (Figure 11). Each of the solutions was kept in a 50°C oven at atmospheric pressure for at least two days to ensure total dissolution of the polymer and dye into the solvent.

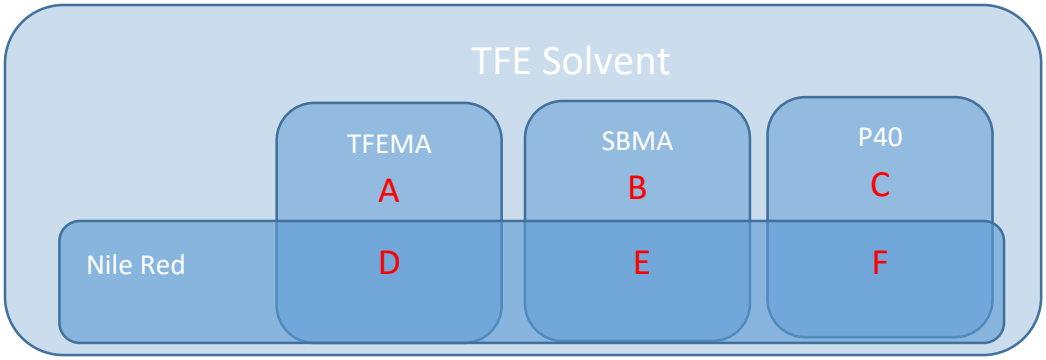

Figure 11: Combinations of polymer, solvent and dye used to create the solutions for Nile Red absorbance tests.

When all six polymer solutions were fully dissolved, they were used to coat the viewing pane of a poly(Methyl Methacrylate) (PMMA) cuvette for use in an Ultraviolet/Visible Spectrometer. When the coating was complete, the TFE solvent was evaporated from the solutions as the cuvettes were stored in a vacuum oven (50°C, -60 cmHg) for at least two days. Once drying was complete, the cuvettes were left coated with a dry, thin coating of the polymer and (in the cases of solutions D, E, and F) Nile Red. The absorbance spectrum of each Nile Red solution was measured from 190 nm to 1100nm and subtracted from its non-dye counterpart so that the spectrum of the polymer and cuvette material could be discounted and only the absorbance of the dye shown. It was necessary to create a polymer solution coating which was as thin as possible because previous attempts to conduct this analysis with thicker coatings resulted in absorbance spectra which contained readings which were at the maximum readable limit of the machine, indicating that there may have been significant sections of the spectrum whose data was not recorded as it was outside the capabilities of the spectrometer.

3 Results and Discussion

The main thrust of this report is concerned with the ways in which the selectivity of thin film composite (TFC) membranes that rely on the self-assembly of zwitterion-containing polymers for the formation of effective pores can be altered easily in the manufacturing step. This would allow for the simple creation of membranes for custom applications, and without the need to run a new synthesis reaction for each application. The way we have chosen to implement these changes is by the addition of small molecules into the casting solution. This an easy change to make to the membrane manufacturing procedure because existing batches of the polymer can simply have the small molecules added to them in solution.

While the use of PTFEMA-*r*-SBMA as TFC membrane selective layers has been reported [3], the alteration and tuning of its selectivity have not yet been explored. In this work, we aim to achieve this by using additives blended with the copolymer during the formation of the selective layer. Specifically, we expect these additives to alter the spatial organization of zwitterionic groups within the membrane nanochannels, and alter membrane selectivity through a molecular imprinting mechanism that would improve the passage of specific compounds similar to the additive used without altering the rejection of others.

To understand the effects that this would have on membranes made from this polymer dope, we begin our investigation by probing the way this addition alters the physical properties of the polymer in bulk. Once we established this, tests were conducted to elucidate the interplay of the additive molecules with the polymer when it is used to make thin-film composite membranes. To begin with, it is necessary to solidify our

knowledge of how the addition of small molecules may be changing the self-assembly of the copolymer material, and specifically, how such small molecules may be segregating themselves within the microphase-separated structure of the bulk polymer.

3.1 Characterizing the Partitioning of Small Molecule Additives Between Domains

3.1.1 Nile Red Absorbance

As a first approach to determining which domains a small molecule additive partitions into when used as an additive in P40, we used a dye whose UV-visible absorbance spectrum changes depending on the polarity of its surroundings, Nile Red. Nile Red's absorbance is different depending on the dipole moment of the environment [68]–[70]. This special property allows us to establish whether the dye has partitioned itself to the hydrophobic or hydrophilic microphase using only the UV-visible absorbance spectrum displayed by it upon mixing with the copolymer. This gives us an easy way to estimate where the dye molecule is positioned within the microphases of the copolymer using only visual clues and quantitative absorbance data from UV-Visible spectroscopy.

In order to elucidate the way additive molecules may be selectively partitioning to the individual microphases within the copolymer, attention was turned to a new additive with especially useful absorbance properties: Nile Red. The Nile Red molecule is unique among dyes in that its light absorbance properties are affected by the polarity of the solvent in which it is present. This property was leveraged as a way to use the absorbance spectrum of copolymer samples cast with Nile Red to determine if the additive was segregating into the highly polar SBMA domains or the hydrophobic TFEMA

microphases. The Nile Red molecule itself is nonpolar and consists of a network of aromatic and heterocyclic rings with a diethylamine functional group.

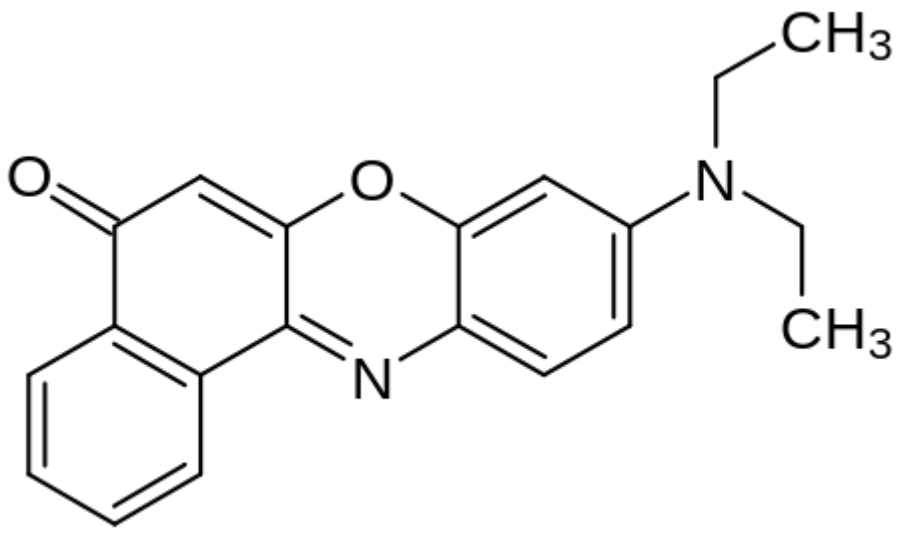

Figure 12: Chemical structure of Nile Red (public domain).

When the Nile Red molecule is in a non-polar solvent, it retains the shape displayed in Figure 12. When the molecule is solvated by a polar solvent, the diethylamine moiety rotates by 90° [68]. With this conformational change, the fluorescence and absorbance of Nile Red changed dramatically (and visibly), allowing both qualitative and quantitative observation to indicate the polarity of the environment around the molecule [68]–[70]. In the system discussed here, the spectral profile displayed by the Nile Red dye in the copolymer may tell the polarity of the polymer which is "solvating" the dye, and therefore, which microphase it has separated into. Though Nile Red is not one of the dyes used in molecule imprinting studies, knowledge of where this additive molecule ends up within the copolymer structure can be indicative of where other additives may go as well. To this end, studies on the segregation behavior of Nile Red were carried out as an analogy to studies into the segregation of Vitamin B12, Direct Red, and other potential

additive molecules which do not have such distinct and recognizable indicators of their environment.

To determine which phase of the PTFEMA-*r*-SBMA copolymer Nile Red was partitioning into, we prepared thin films of the copolymer, PTFEMA homopolymer and PSBMA homopolymer with and without Nile Red. Then, these films were tested for their absorbance spectra. In conducting these comparative tests, evidence of selective segregation of Nile Red to one microphase would come in the form of a spectrum in the copolymer which was markedly more similar to the spectrum of one of the homopolymers.

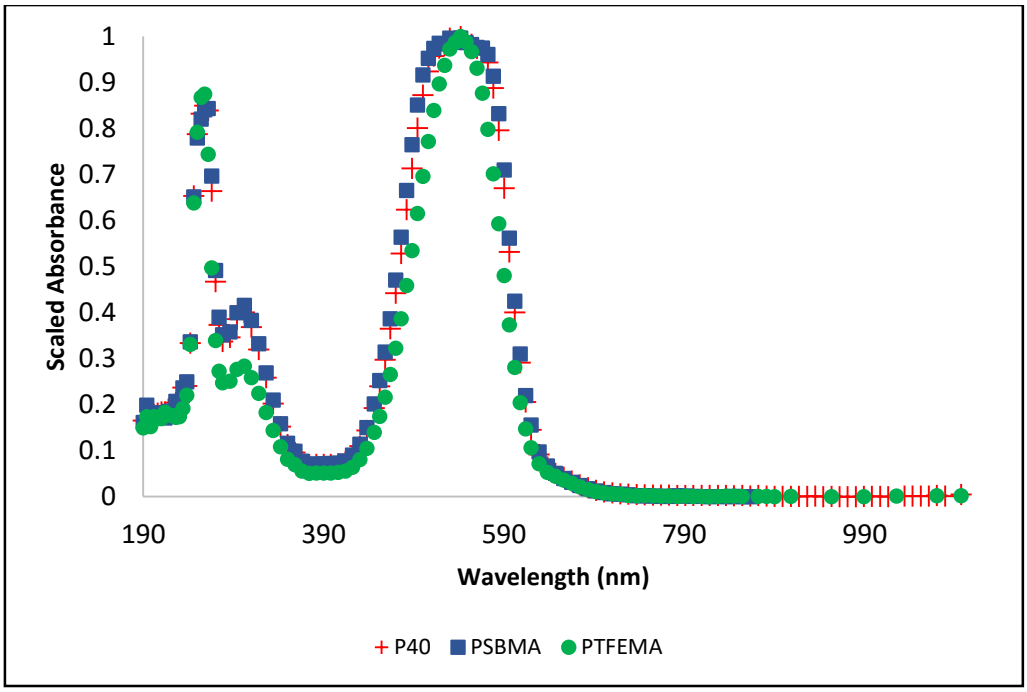

Figure 13: Absorbance spectra for TFEMA and SBMA homopolymers and P40 copolymer. In each case, the absorbance of solutions made without dye is subtracted as baselines.

Figure 13 shows the absorbance of Nile Red in each of the homopolymers and the copolymer. The value of absorbance at each wavelength has been normalized such that the highest reading is denoted as having a value of 1 and all other absorbance data

represent a fraction of the maximum to allow for easier comparison between data sets and eliminate variations due to inconsistencies in the thickness of polymer films. Each of the spectra exhibits three absorption maxima. The first maximum occurs at 256nm where each plot approaches a value of 1 indicating that each is nearing the highest absorbance value obtained in its entire spectrum. The second minor peak is displayed at approximately 300nm and shows a much higher absorbance in the TFEMA homopolymer solution than in the SBMA homopolymer or the copolymer. The final maximum occurs at 545nm. The absorbance of wavelengths around the maxima displayed in Figure 13 shows that there is a much better agreement in absorbance spectra of Nile Red in SBMA and in the copolymer. the spectrum of Nile Red in TFEMA follows a different pattern. Nile Red in both SBMA solution and P40 have a significantly stronger absorbance at 545 nm, whereas Nile Red in the TFEMA film does not show as high a relative absorbance at this wavelength. Overall, there is a better agreement between the relative sizes of the peaks for Nile Red in the P40 copolymer and the SBMA homopolymer. This indicates that Nile Red likely segregates into the SBMA zwitterionic phases preferentially, though that does not exclude the possibility of some less prominent segregation into the TFEMA microphases.

An important consideration of this work is that Nile Red can only be used as an analogous compound to give an indication of the segregation behavior of the other additive molecules considered here. The interpreted behavior of Nile Red can give a good approximation of the segregation of other additives, but it is important to note, that it is only a first approximation. Having knowledge of the microphases that Nile Red segregates into is helpful for estimating where other additives may go when they are introduced into

the casting solution before solidification, but it cannot give information on the behavior of the other additives used, such as Vitamin B12 or Direct Red 80.

3.1.2 Characterization of Copolymer-Vitamin B12 Interactions by Thermal Analysis

The first additive molecule investigated was the cyanocobalamin variant of the Vitamin B12 molecule. Vitamin B12 was selected as an additive candidate because of its interesting electronic characteristics, its large size and its high solubility in water (as high as 1.25×10^4 mg/L) [71]. Vitamin B12 is a zwitterionic molecule, with charge distribution between the nitrogen atoms in the corrin ring conjugated with the large cobalt ion (positively charged) and the phosphate group (negatively charged) within the organic portion of the molecule. The molecule also has a large region of hydrophobic carbon architecture. Thus, the zwitterionic nature of the molecule can enable it to interact with the zwitterionic groups of SBMA due to the high dipoles, providing strong interaction forces that arrange the functional groups as the polymer solidifies to form the selective layer.

The effects of Vitamin B12 additive upon the structure and morphology of the membranes was investigated using thermal analysis. It was hypothesized that adding small molecules with similar chemical structure and polarity to one of the microphases (i.e. SBMA) in the copolymer could create a situation where the additive molecule selectively segregates itself into only those domains. This could cause the plasticization of only those domains, as demonstrated by a decrease in the glass transition temperature (T_g) measured by thermal analysis methods if the segregating molecule also increased the mobility of the polymer segments in that domain. In this case, the zwitterionic Vitamin

B12 could interact with the zwitterionic SBMA pendant groups to alter the thermal mobility of those groups, potentially leading to a lower T_g value for the SBMA phase in comparison with the pure copolymer. To establish if this was the case, Modulated Differential Scanning Calorimetry (DSC; TA Instruments DSC Q100 V9.9 Build 303) was employed to show the T_g values in samples cast with and without small molecule additives. PTFEMA homopolymer has a glass transition at about 74°C [72], while the zwitterionic polymer PSBMA has a glass transition at around 181°C [73]. However, because of the very small domain sizes and the highly interconnected nature of the microphases within this copolymer, as long as one of the segments remains glassy and immobile, the DSC instrument may not be able to detect thermal property changes that result from the mobility of the other phase. This means that the PTFEMA glass transition temperature may be difficult or even impossible to observe accurately using this method as the glassy nature of the PSBMA would constrain chain motion even in the PTFEMA phase at this temperature and prevent thermal transitions from being observed [74]. However, the T_g of the PSBMA phase should be measurable as its T_g is at a larger temperature than that of PTFEMA.

Figure 14 shows the reversible heat flow in samples with and without Vitamin B12 additive over a wide temperature range. All three samples show glass transition temperatures around 181°C, similar to that of the PSBMA homopolymer. No glass transition is seen around 74°C, confirming that the SBMA microphases are indeed obscuring the observability of the thermally induced motion of TFEMA.

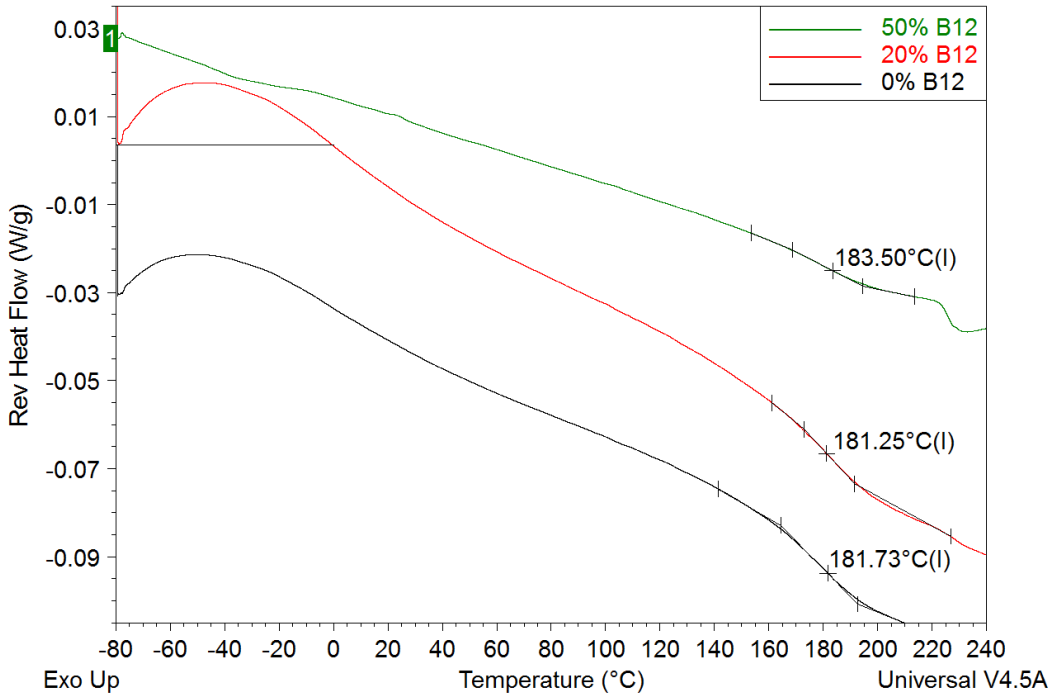

Figure 14: Differential Scanning Calorimetry results for a modulated temperature profile.

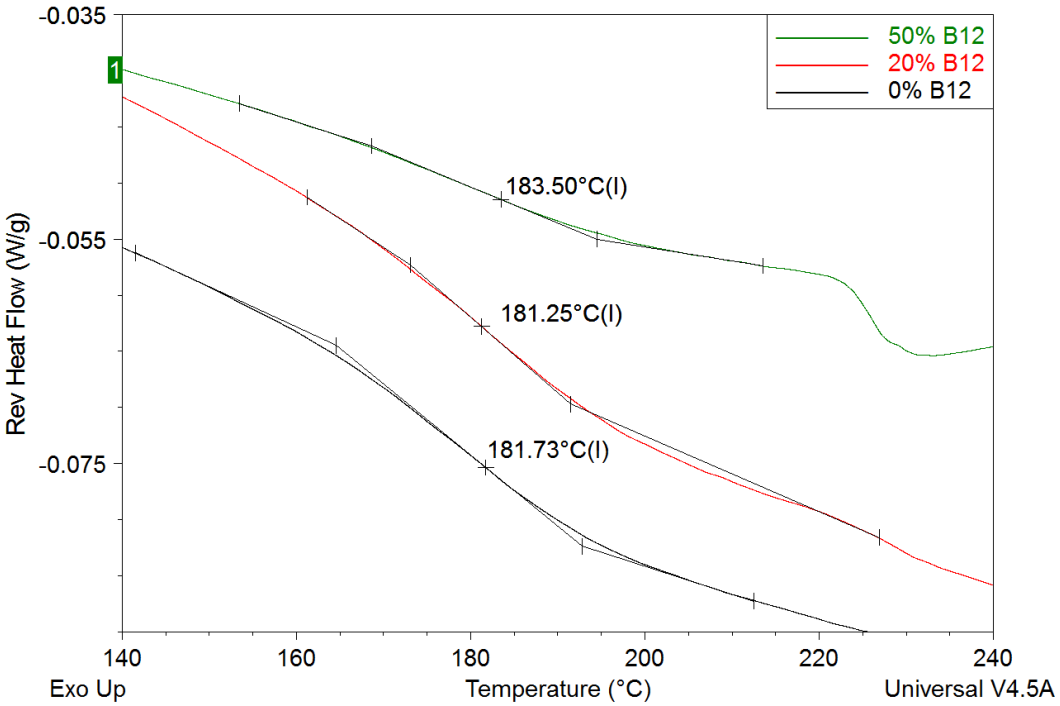

Figure 15: Differential Scanning Calorimetry results for modulated temperature profile, close-up view of glass transition region.

The section of the DSC analysis where glass transitions are observed is seen in more detail in Figure 15 which represents a close-up view of the same data set as in Figure 14. When Vitamin B12 is added to the polymer casting solution from which DSC samples were made, no change in the location of the glass transition is observed. This indicates that there is likely no selective plasticization of the SBMA phase. Furthermore, it indicates that Vitamin B12 does not increase the chain mobility in SBMA domains. These results could be explained by Vitamin B12 not segregating into the SBMA domains. However, other observations make this explanation unlikely. Vitamin B12 is indeed most similar to the SBMA domains chemically, especially given its zwitterionic nature. Furthermore, past research indicates that solidified P40 copolymer includes SBMA domains permeable to water, and hydrophobic PTFEMA domains. If Vitamin B12 had segregated into PTFEMA, it would be impossible to leach it from solidified polymer by placing it into water. However, we have observed that when P40 is blended with Vitamin B12, cast and then immersed into water, Vitamin B12 can be removed effectively provided sufficient time is given for these large solutes to diffuse out. Thus, we expect Vitamin B12 to be located within the SBMA domains.

Combined with the unchanged T_g, however, these results indicate that Vitamin B12 goes into the SBMA domains but does not improve chain mobility. This could arise from strong interactions between B12 and SBMA, similar to the strong dipole-dipole interactions between the SBMA units. The large molecular size of Vitamin B12 also implies limited molecular mobility. As both molecules are zwitterionic, this hypothesis is plausible, though it needs further exploration.

3.2 Performance of Membranes Cast with Small Molecule Additives

Typically, filtration membranes are classified by the molecular weight cut off, that is the weight at which 90% or more of a feed molecule is rejected [13], or where 95% of a globular protein of equal weight is rejected (so as to eliminate effects of molecular geometry) [1]. Generally, molecules of varying sizes can be filtered in succession to determine at what diameter they are no longer able to pass easily through the membrane's pores. Such a procedure produces a chart known as a rejection curve which depicts the size of filtrate molecule at which a transition occurs between passing through the membrane to being retained in the upstream reservoir. In this case, however, a more accurate prediction of channel size was desired than can be established by the correlation of molecular weight with size. Therefore, it is necessary to construct a rejection curve using a direct estimate of the size of each challenge molecule as opposed to their weight. To this end, Molecular Modeling Pro software was used to estimate the size of each molecule filtered. While this is a more accurate estimation of size than molecular weight, it bears noting that this program is known to underestimate size by neglecting the size contribution of a hydration shell.

3.2.1 Manufacture of P40 TFC Membranes with Vitamin B12 Additive

As discussed above, Vitamin B12 was the first additive candidate investigated in this study due to its zwitterionic nature and its size comparable to the effective pore size of the membrane. The structure of Vitamin B12 is shown schematically in Figure 16. To prepare these membranes, we blended the PTFEMA-r-SBMA copolymer with varying amounts of Vitamin B12 in the coating solution. The solution was then coated onto PVDF base membranes which provide mechanical support without interfering with the separation ability of the thin film coating. In this study, we used Vitamin B12

concentrations that were 0%, 20% and 50% of the weight of the copolymer in the casting solution, to determine if there was an optimal amount of additive that led to the molecular imprinting effects. This was intended to show whether there was a correlation between the amount of additive and the degree to which filtration alteration took effect. Solutions with Vitamin B12 equivalent to 50% of the copolymer had roughly equal amounts of SBMA and Vitamin B12 by mass.

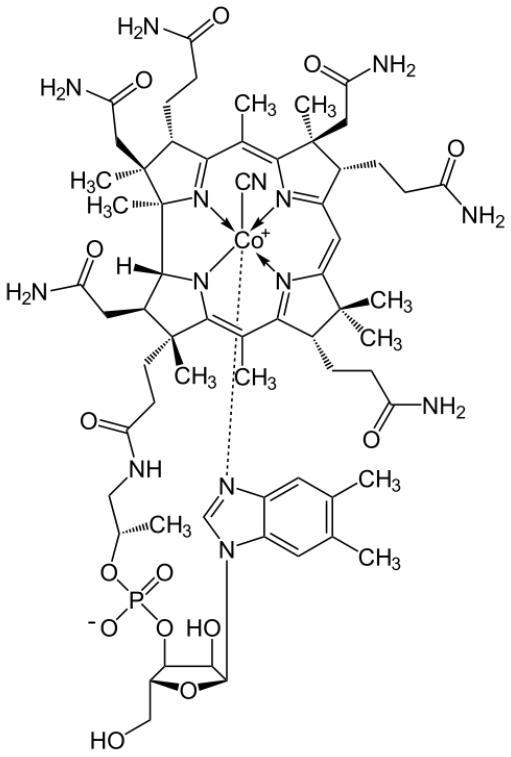

Figure 16: Structure of cyanocobalamin Vitamin B12 molecule (Public Domain).

The morphology of the membranes created is a special concern for the applicability of this technology in a commercial role, as it may affect the permeance. Some example SEM images of membrane cross-sections are given in Figure 17 for each Vitamin B12 concentration. The TFC membrane morphology and the presence of a thin, dense

copolymer selective layer are the most important aspects of the membrane observed in this way. Figure 18 shows that there is no significant trend between the amount of Vitamin B12 in a casting solution and the thickness of the selective layer made with that solution. It is well established that the factors influencing coated thickness of a thin-film composite membrane are numerous, and include such considerations as temperature, humidity, and evaporation rate of solvent [33]. Because the thickness at each B12 content is roughly the same on average, and because there is a large range of thicknesses displayed, these other factors are likely at play and dominate the influence of the thickness of the selective layer.

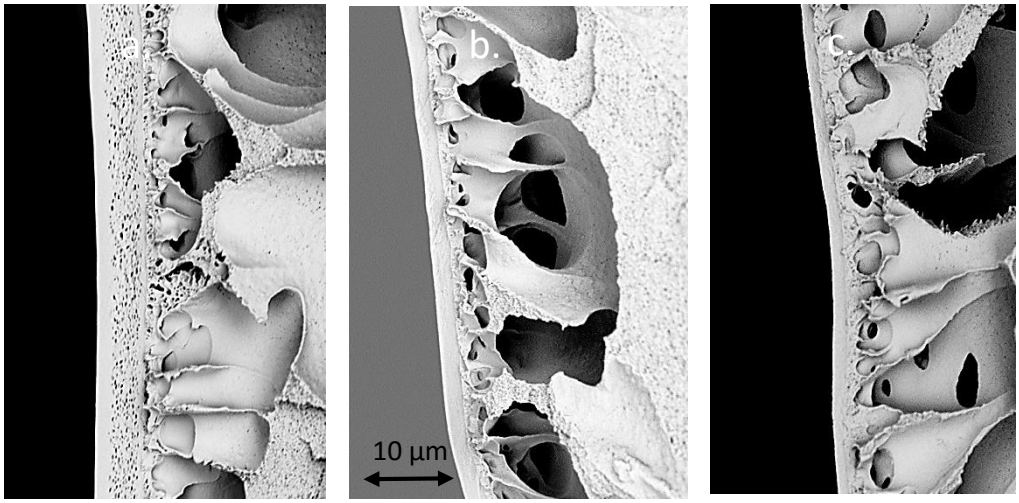

Figure 17: SEM micrographs of: a. 0% additive membrane, b. 20% B12 membrane, c. 50% B12 membrane. All images were taken under 5000x magnification.

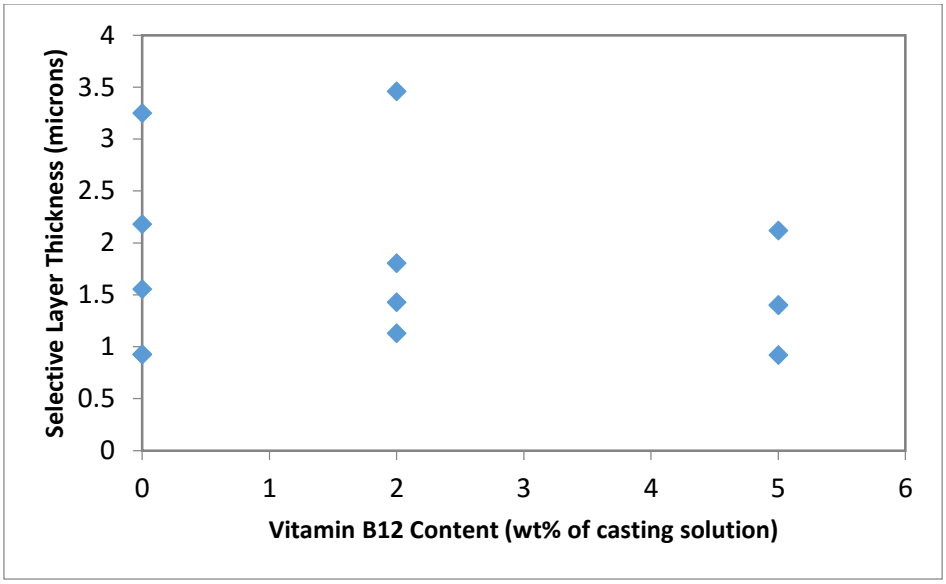

Figure 18: The thickness of each selective layer made, displayed as a function of the weight percent of Vitamin B12 in the casting solution.

While we see no trend between the amount of Vitamin B12 additive in a membrane and the film thickness of that membrane, we might expect a secondary trend to present itself: a trend between the thickness of the selective layer and pure water permeance, because the flux through a membrane can be modeled as inversely proportional to its thickness [1], [16], [17]. Interestingly, in membranes made using Vitamin B12 as an additive, we see no such correlation. Figure 19 shows that the expected trend of lower water flux with increasing thickness is not displayed for the membranes manufactured with Vitamin B12 additives for this study. For this plot, the thickness was taken as an average of at least three thicknesses measured from the same image, to give a representative thickness for a membrane swatch. The water flux was calculated using the measured filtrate weight from the first at-pressure water filtrations performed on each swatch. From these results and the results of the comparison between additive content and thickness, we conclude that for this system, the coating thickness or additive content do not dominate the resultant water permeance. In many cases, it was observed

that the polymer solution penetrates into the pores of the base membrane due to capillary forces rather than forming a layer only on top. This can cause pore clogging within the sublayers of the membrane, causing permeance loss without corresponding gains in selectivity. This effect is believed to cause significant contributions to the observed variability in permeance. Potentially, this can be prevented by better selection of a base membrane and optimization of coating parameters. However, this was not the focus of this thesis.

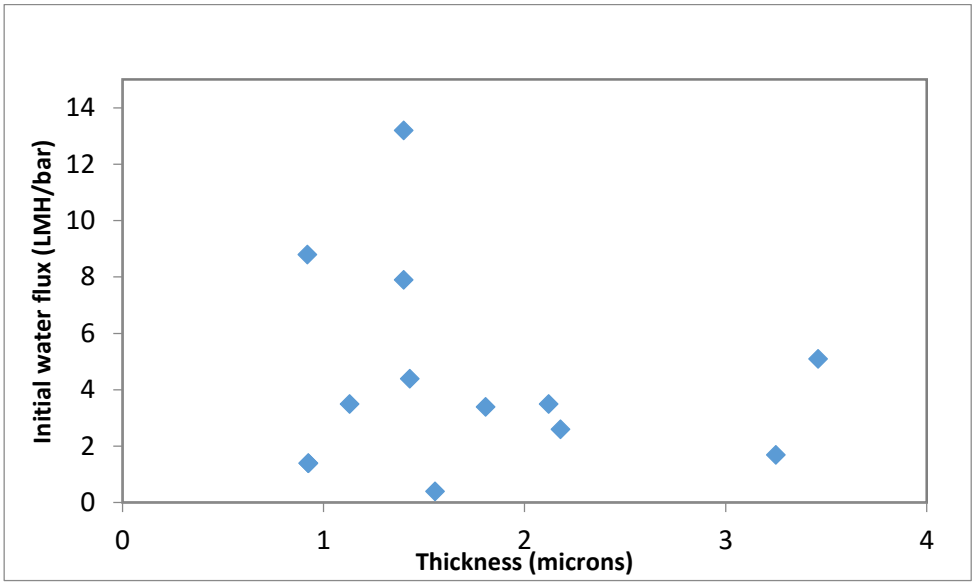

Figure 19: Water flux in membranes cast with Vitamin B12 versus the thickness of the selective layer as established by SEM.

Given this manufacturing scheme, water solubility is an important feature of an additive molecule. We require the additive to remain present in the isopropanol casting solution while the channels are forming in the coagulation bath, but for it to be completely washed out of the polymer in water before filtration tests are run. If the additive leaves the polymer structure before the channels are formed, the imprinting would not be possible as the structure would stabilize in the absence of any interacting molecules. If the additive does not wash out completely before membrane testing, it may

prevent us from measuring stable rejection properties by partially clogging either the channels or interacting functional groups. In the case of a colored compound like Vitamin B12, this would also interfere with future measurements of rejection, as our selectivity characterization method relies on measuring the rejection of various dyes (including Vitamin B12) by UV/visible spectroscopy, where the presence of additive in the filtrate could cause inaccurate absorption spectra.

Interestingly, while we see no trend between the additive concentration and thickness, nor between thickness and water flux, there does appear to be a trend when we consider the relationship between additive content and water flux. Figure 20 shows that the water permeance during the first water filtration after compaction increases as more additive is introduced into the casting solution. In this plot, the error bars represent the deviation observed upon reproducing the permeation tests. As discussed above, the permeation rate of membranes is calculated using automatic, computerized data collection which yields very precise data for each filtration conducted. This is an interesting result because the permeance of a membrane is a key factor determining the speed by which a membrane can carry out its filtration workload. A faster-working membrane, therefore, decreases the operating time and cost associated with maintaining the operating pressure on the feed solution.

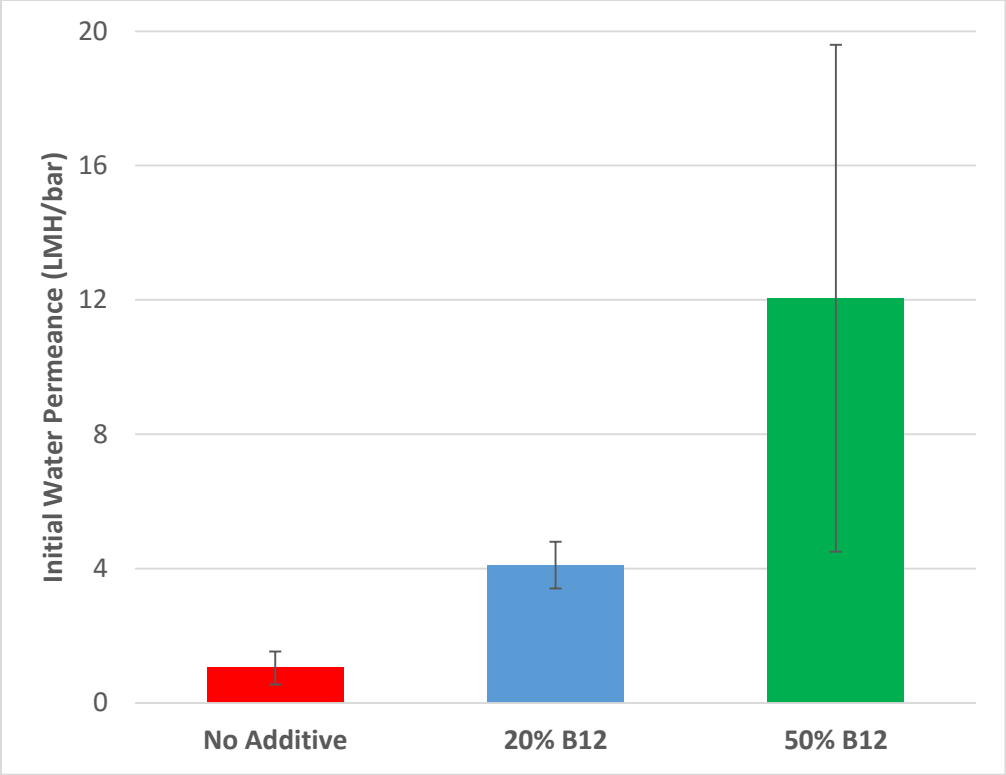

Figure 20: Initial water permeation rate through TFC membranes cast with various amounts of Vitamin B12 additive.

To establish if Vitamin B12 was being washed out from the coagulated polymer into the filtrate volume, we collected fractioned volumes from the filtrate during the membrane's initial compaction by filtering deionized water through the membrane after manufacture. If B12 were able to fully dissociate in the water bath, we would clearly expect there to be no residual dye in the filtrate when pure water is used as the feed. As can be seen in Figure 21, however, a small amount of Vitamin B12 was still observed in the permeate. While most Vitamin B12 was removed during casting, a small amount of Vitamin B12 remained, and washed out during water filtration, aided by convective flow. Figure 21 shows the concentration of Vitamin B12 in the initial water filtrate as a function of time as established by UV/visible spectroscopy. It should be noted that the points corresponding to 0.05 PPM of B12 represent the lower limit of detection for the

spectrometer employed here. Based on these time-dependent results, we conclude that while there may be a minuscule amount of additive molecule which does not diffuse out of the polymer freely, the amount that is left is continuously decreased in the initial stages of filtration tests (before dye concentration is measured). The amounts of Vitamin B12 observed to wash out are also extremely low, and the addition of this amount to a filtrate sample would not create a statistically significant change in the concentration measured in the filtrate.

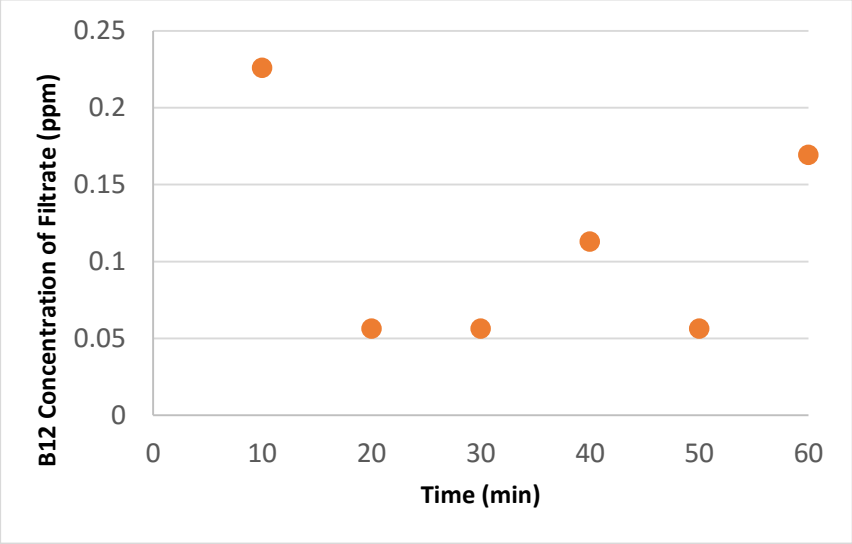

Figure 21: Time evolution of additive content in water compaction filtrate for a membrane cast from a solution containing 50% Vitamin B12.

To analyze the effect of this additive on the overall effective pore size of the membrane, a series of anionic dyes varying in size from 0.79 to 1.3 nm were filtered through the membranes prepared with Vitamin B12 additive (at 20% and 50% of polymer mass). No significant difference was observed in the effective size cut-off as compared to membranes cast with no additive, including membranes prepared with the same polymer batch (Figure 22) and those prepared by Bengani et al. using a different batch of the same copolymer composition [3]. All membranes, prepared with or without the Vitamin B12

additive were able to almost fully reject anionic dye molecules with a calculated hydrodynamic diameter greater than 1.1 nm. Previous studies have established that a membrane of unmodified copolymer displays size-based exclusion regardless of charge [3]; this property is also seen in the additive-containing and additive-free polymers prepared for this investigation.

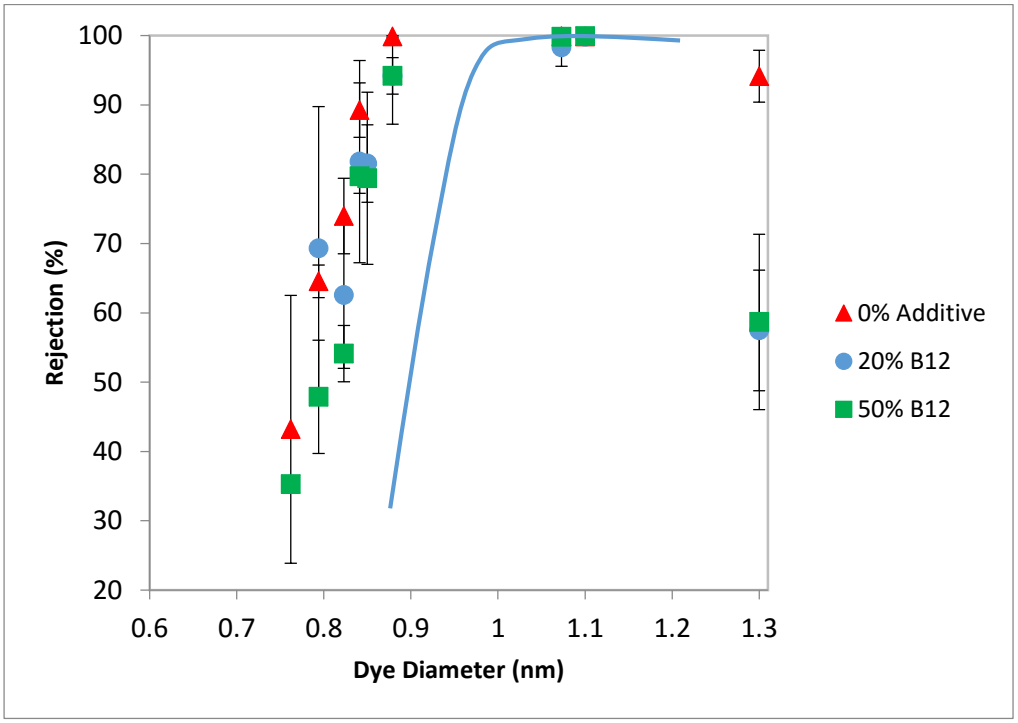

Figure 22: Effect of size-based separation of Vitamin B12 concentration in casting solution. The data at 1.3nm represent the rejection of Vitamin B12 solutes. Error displayed here results because each rejection point is the average of the rejection of at least three filtration tests carried out on different membranes. Blue curve added to highlight the rejection trends.

In each of the rejection curves prepared for each of the B12 additive samples, the rejection value for the B12 molecule itself (displayed at 1.3 nm in Figure 22) appeared aberrant. The rejection of Vitamin B12 was significantly lower for the membranes prepared using the Vitamin B12 as an additive compared with the membranes prepared without. The value for the 20% and 50% B12 membranes also varied substantially (between 46 and 67% rejection in the 20% B12 sample, and between 43 and 82% in the

50% B12 case). This disparity was not observed in the B12 rejection behavior of the additive-free samples tested. These results support the hypothesis that the Vitamin B12 additive modifies membrane selectivity through a molecular imprinting-based mechanism, where interaction sites specific to Vitamin B12 left behind during membrane formation increase the passage specifically of this solute, possibly by increasing the partitioning of Vitamin B12 into the membrane selective layer.

It is worth mentioning that the rejection observed for solutions of Vitamin B12 in the unmodified membrane is slightly lower than might be expected given its size. This drop occurs in many of the filtration data sets presented here and is attributed to some inaccuracy in the molecular modeling which was used to calculate the size of the Vitamin B12 molecule, which is less rigid than the anionic dye molecules used as probes here. Because of the shape of the molecule, it is hypothesized that certain conformations of Vitamin B12 can allow the molecule to fit through a pore to a small degree. The B12 molecule is known to have two rigid sections connected by a flexible segment. It is possible that the flexible portion of the molecule is allowing Vitamin B12 to change its conformation in response to the induced pressure to fit more easily through the pores in the membrane. If this is the case, it does not appear that the deviation in rejection because of this conformational fluidity represents a change of more than a few percentage points, and therefore does not cloud the statistically relevant deviations observed for molecular imprinting.

A potential alternative cause of the observed drop in Vitamin B12 rejection in membranes modified with Vitamin B12 as the imprinting agent could be a slow washout of the additive used in membrane preparation, as opposed to actual passage of the solute through the membrane. Because so much Vitamin B12 was used in the membrane during

the casting stage (up to 50% of the polymer by mass), the reduced rejection data shown here could be interpreted as residual additive still present within the membrane being washed out. This explanation would be predicated upon an assumption that the additive Vitamin B12 was not fully washed out in the DI water stream due to solubility limitations. That is to say that the initial compaction carried out with DI water was not able to wash out Vitamin B12 because the dye was not as soluble in DI water as it would be in the ionized water solvating Vitamin B12 feed solutions. This would lead to a situation where the Vitamin B12 additive could be contained within the polymer structure, unable to be liberated until it comes in contact with water containing appropriate counterions to aid in solvation. However, Vitamin B12 is known to have a high water solubility, and the similarity in pH between the Vitamin B12 solution (~6.5) and the DI tap water (~5.5) lead to the refutation that any remaining B12 skewed the rejection data. Thus, the imprinting B12 was most likely washed out fully in the water flushes carried out before dyes were filtered and measured, the results of which are shown previously in Figure 21. This is observationally confirmed by the lack of distinct pink coloration in the dye-laden membranes which would be indicative of the presence of Vitamin B12.

3.2.2 Manufacture of P40 Membranes Using Other Small Molecule Additives

In order to check for the effect of molecular imprinting, we also investigated the addition of the dye Direct Red 80 (DR80) to the casting solution. This was done to test whether any solute we selected could be allowed to pass through the membrane by having it present in the casting solution from which the membrane was manufactured, or if this molecular imprinting effect was particularly successful with specific families of solutes. Direct Red 80 was chosen for this purpose because, with a molecular diameter of approximately 1 nm, it is about the same size as the other imprinting candidate used here,

Vitamin B12. If DR80 preferentially segregates into the zwitterion domains in the copolymer, interacts with the zwitterionic groups to spatially arrange them in a way that leads to preferential binding sites, and remains in place while the polymer hardens in the coagulation bath, it is possible that its rejection, like that of Vitamin B12, will decrease while the rejection of other solutes remains the same. This dye contains six sulfonate groups at various locations along the molecule which results in an overall 6- charge which is countered by sodium ions. The high degree of charging in this dye is not required to achieve the pigment optical properties, but is imposed to aid in water dissolution and may, for our purposes, aid in the segregation of this molecule to the sulfobetaine groups along the copolymer in the nascent membrane. DR80 was also selected to test for molecular imprinting because it showed very high rejection in baseline filtration tests. Because the rejection of DR80 was always approximately 100% in unmodified membranes, it would be easy to see the effects of molecular imprinting, as this would result in a low rejection for the imprinted molecule and normal rejection for solute molecules of similar sizes.

The results of rejection tests performed on membranes cast in this way are shown in Figure 23. Direct Red 80 rejection (located at a diameter of 1.07 nm) fits well onto the S-shape size-based rejection curve when no additive was used in the casting solution. In the case where Direct Red 80 is added to the casting solution, the membranes show the same selectivity behavior as in the additive-free membranes, corresponding to an effective pore size of 0.8-1 nm. Direct Red 80 rejection remains unchanged. While there is some fluctuation in the Vitamin B12 rejection, located at a diameter of 1.3nm on the curve, the change is relatively minor and likely within the error margins observed for the

rejection of this specific solute. It is definitely less prominent than the rejection observed when Vitamin B12 is used as the additive.

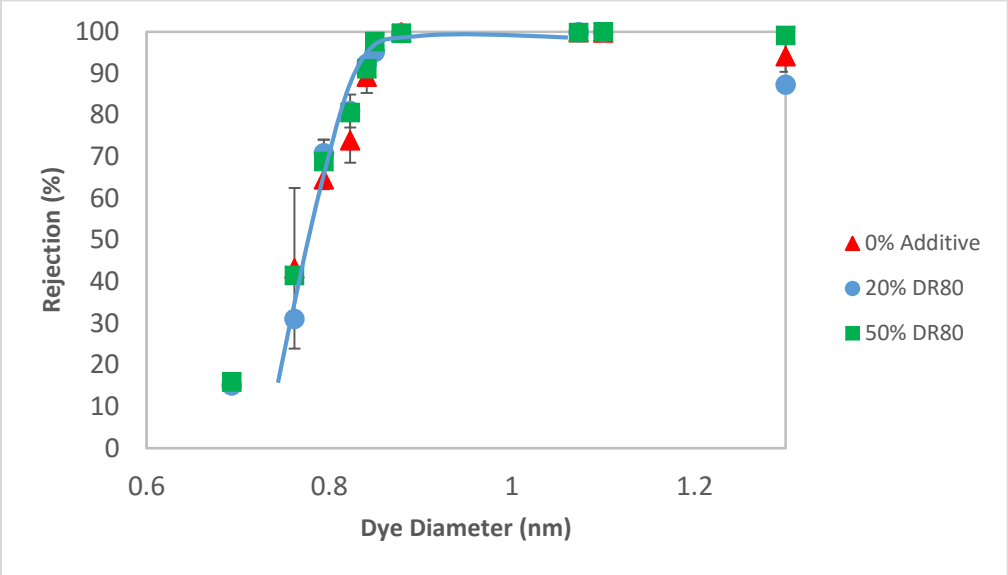

Figure 23: Filtration results from membranes cast with various amounts of Direct Red 80.

As with the membranes cast with Vitamin B12, those created using Direct Red 80 as an additive were investigated for trends between the inclusion of the additive and changes in the flux of the resulting membranes. Figure 24 shows that unlike membranes cast with Vitamin B12, those cast with Direct Red 80 show no trend of increasing water permeance with increasing additive concentration. Because each of the data corresponding to additive-containing membranes relies on the results of only one test, it is likely that the increase in flux between 0% additive and 20% additive, and the subsequent flux loss upon addition of more additive is not a true trend but an artifact of these particular data.

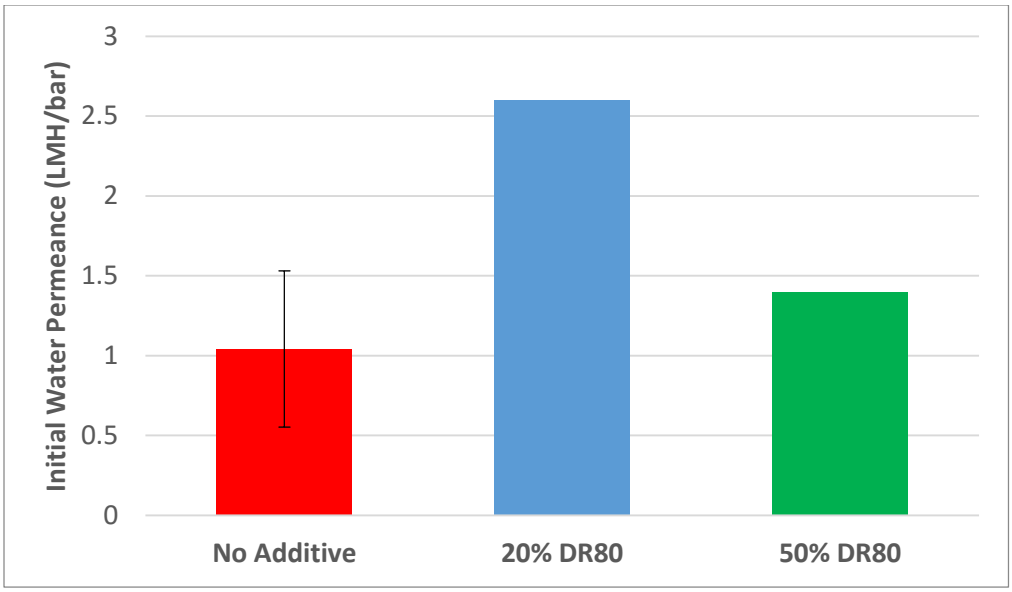

Figure 24: Initial water flux of membranes cast with Direct Red 80 additives based on the concentration of additive they contain.

We also wanted to use an additive molecule that was as chemically similar to the non-glassy zwitterion sections of the polymer which make up the channels in the membrane. Therefore, another small molecule additive tried was the zwitterionic monomer used in the copolymerization, sulfobetaine methacrylate (SBMA). As with the other additives, SBMA was added to the casting solution at two concentrations and filtration data were collected for the full battery of dyes with radii between about 0.8 and 1.3 nm.

Figure 25 shows that the membranes cast with SBMA reject almost all solutes tested to the same extent as the membranes prepared with no additives, exhibiting a size-based cutoff with solutes slightly larger than 0.8 nm. Vitamin B12 rejection appears slightly lower for the membrane prepared with 50% SBMA with respect to the copolymer. This may be due to a weak molecular imprinting effect that preferentially allows zwitterionic solutes, including Vitamin B12, through. As expected, the change in Vitamin B12 rejection is not nearly as significant as that observed when Vitamin B12 was used as

the additive. The imprinting effect is much weaker when a similar solute (as opposed to the actual target compound) is used during membrane manufacture.

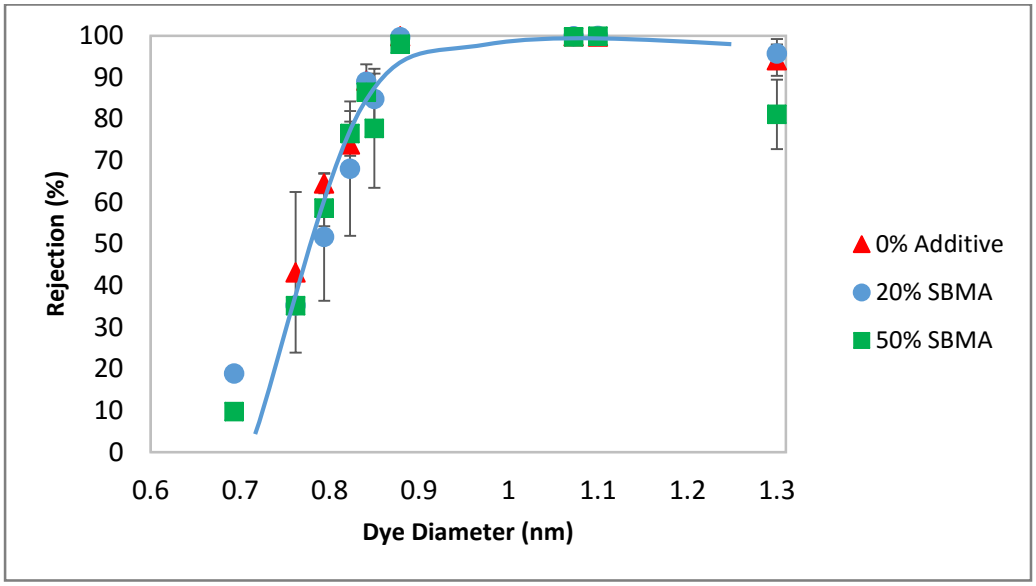

Figure 25: Rejection curve for dyes filtered through membranes cast with sulfobetaine methacrylate monomer additive at various concentrations.

The permeance was recorded and analyzed for the addition of SBMA as it was for the other additives reported here. The results of this analysis are shown in Figure 26 and display what could be interpreted as an increase in initial water permeance with an increase in zwitterion additive concentration. This trend must be considered with caution, however, because only one permeance datum was collected for each of the additive-containing samples. This was because the addition of SBMA was not as major a component of this thesis, as compared to experiments conducted on membranes created with Vitamin B12 and Direct Red 80.

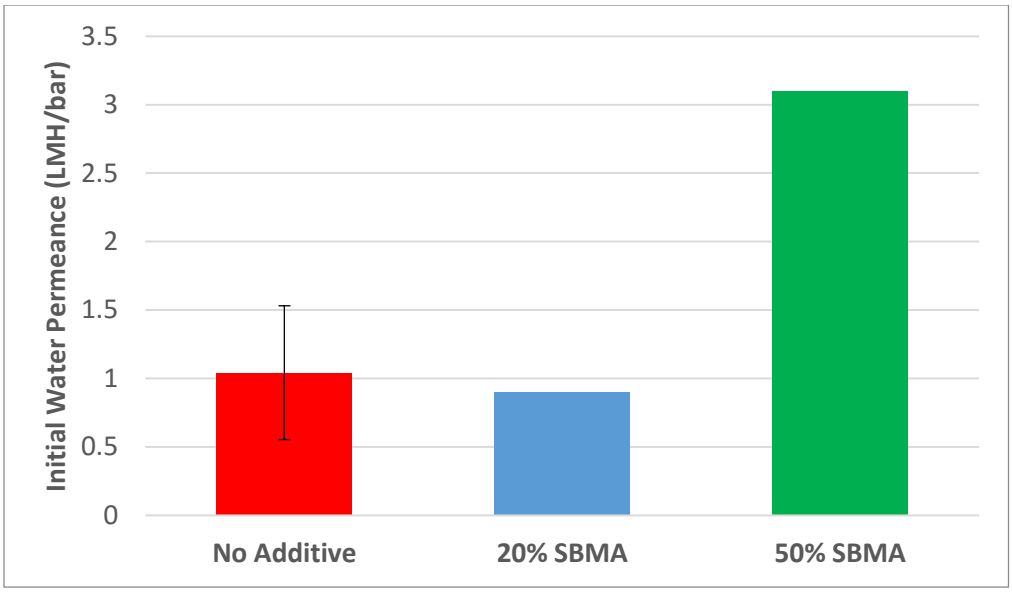

Figure 26: Initial water permeance for virgin dope and for membranes created using SBMA as a small-molecule additive.

In a similar attempt to find additives which have a similar chemical structure to the zwitterion portion of the copolymer, we also investigated the use of a zwitterionic surfactant with similar charge-bearing groups to sulfobetaine. The detergent that was selected was 3-(1-Pyridinio)-1-Propane Sulfonate (PPS) which contains a tertiary amine cation and a sulfonate anion similar to SBMA, as shown in Figure 27. Figure 28 shows that the rejection of most solutes still remains unchanged, with a size cut-off at about 0.8 nm diameter. Similar to the results observed with SBMA, the rejection of Vitamin B12, the only zwitterionic solute tested, shows a minor decline. We hypothesize that, as explained above, this is due to the chemical similarity between PPS and Vitamin B12.

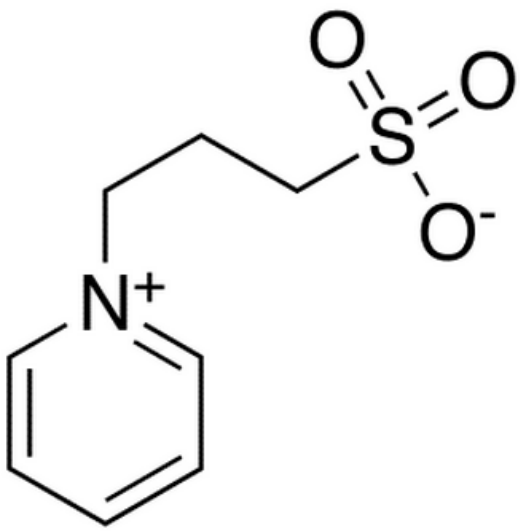

Figure 27: Chemical structure of the zwitterionic additive PPS. (Public Domain)

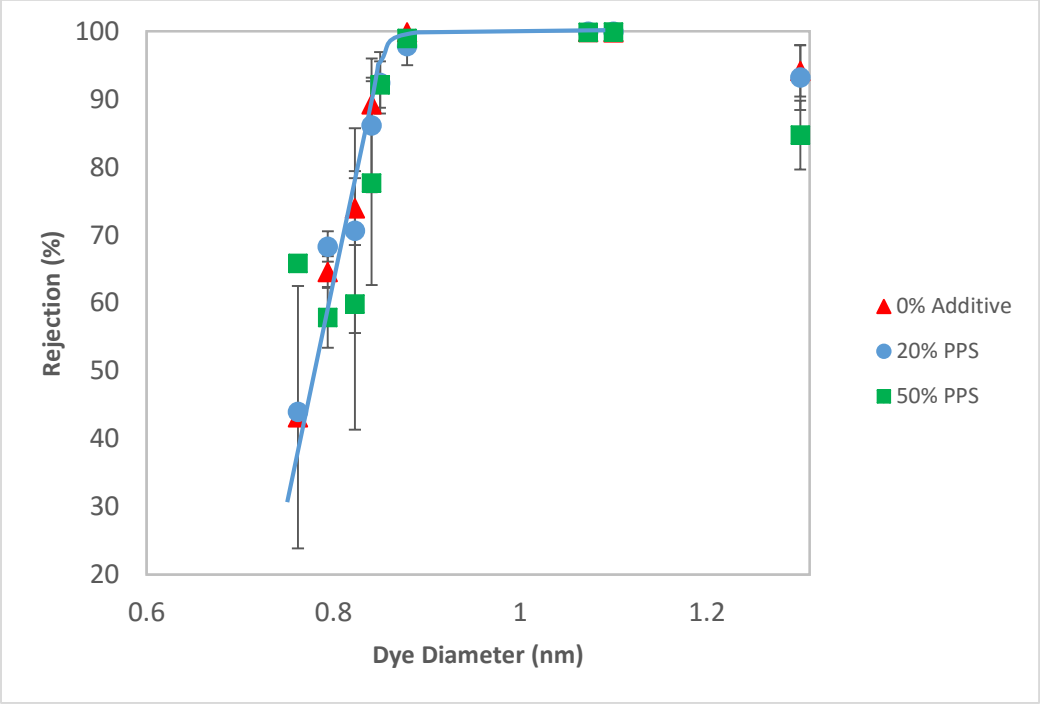

Figure 28: Rejection of various dyes in membranes cast with two concentrations of PPS additive.

It was also possible to test the water permeance of membranes cast from solutions containing PPS against the concentration of PPS which was left in the polymer

selective layer upon solvent inversion. Figure 29 shows the results of this analysis. There appears to be an increase in water permeance when a high loading of PPS is used in the polymer layer, though the error for these data is also much larger. PPS is a zwitterionic solute and it is possible that it is interacting favorably with the zwitterionic microphase in the copolymer. This indicates that as with the addition of Vitamin B12, the identity of the small-molecule additive is a key factor in determining how it affects the behavior of the polymer in various metrics.

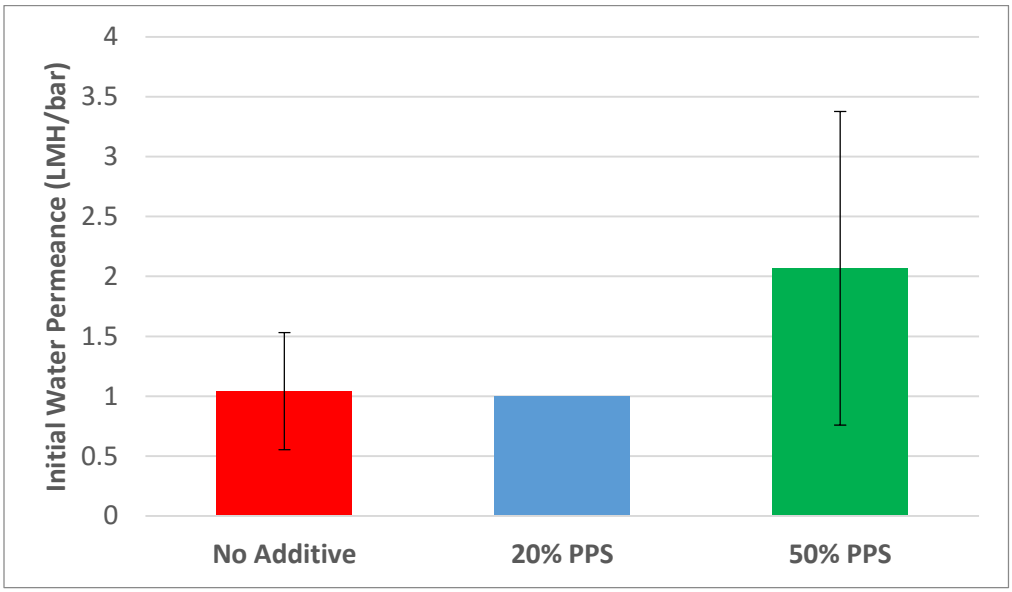

Figure 29: Water permeance as a function of PPS content in the selective layer.

The addition of PPS to the casting solution was also investigated with respect to the physical changes that could result which would present themselves in the thermal properties of the polymer. As with Vitamin B12 additive polymer samples, copolymer made with PPS in the casting solution at various amounts was tested in the Differential Scanning Calorimeter to determine if the small molecule added in this case was plasticizing either of the phases, a change that would be visible as a shifting of the glass transition temperature of the polymer. The same modulated temperature profile was

used to analyze polymer samples made with PPS as was used previously to investigate the addition of Vitamin B12.

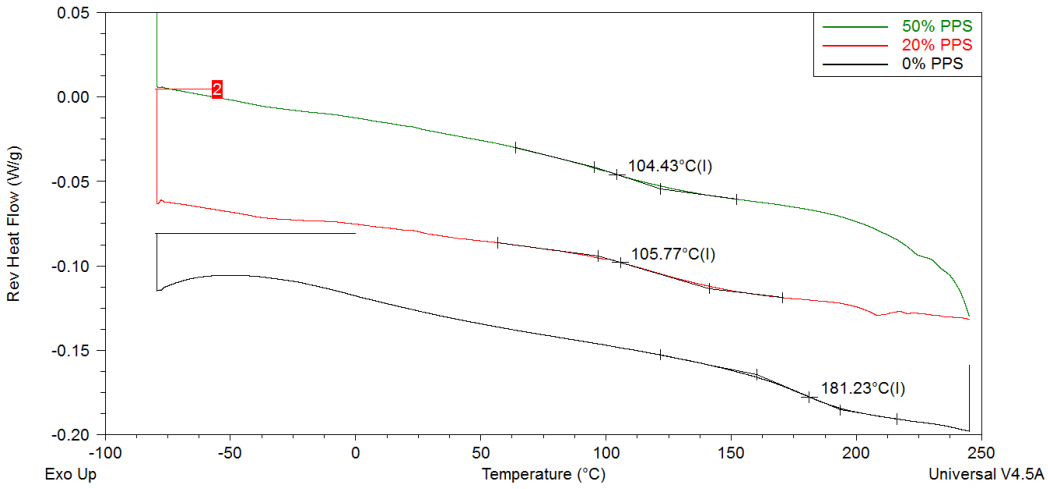

Figure 30: DSC results from polymer samples prepared with various amounts of PPS additive.

As can be seen in the heat flow results shown in Figure 30, there appears to be a significant reduction in glass transition upon the addition of PPS to the polymer casting solution. The drop in glass transition is seen when 20% of the additive is present, and the shift is roughly the same when a higher loading of additive is used. In contrast to the addition of Vitamin B12, this is seen as evidence that the PPS is plasticizing the SBMA zwitterion polymer phase and causing it to be more mobile under thermal stimulation. The efficacy of a plasticizer is derived from its ability to enhance chain mobility. It would appear that the zwitterionic character of PPS allows it to segregate into the SBMA polymer microphase and to alter the mobility of chains in those domains. This serves as more evidence that additives with complementary structures to the zwitterion phase of the polymer can partition themselves to create novel interactions and alter the behavior of the polymer self-assembly at the will of a researcher, a powerful tool for the commercialization of a polymer system.

3.3 Air Drying Before IPA Solvent Inversion

The residence time of the additive during the casting stage is a crucial factor in successful molecular imprinting. The additive needs to remain in the copolymer, keeping the functional groups that interact with it in an optimal spatial arrangement, until the copolymer is fully solidified. This means that if the additive (e.g. Vitamin B12) washes out of the polymer domains before the copolymer has fully coagulated, the imprinting could be left incomplete.

One possible approach to adjusting this residence time is to change the time for which the polymer membranes were left to air dry before immersion in isopropanol. To test if the additive residence time during the proposed manufacturing scheme affects the selectivity of the membranes, the copolymer was coated onto PVDF base membranes and left to dry in the fume hood before being transferred to the IPA bath. Noticeable drying could be accomplished in relatively short time spans because of the high vapor pressure of the polymer solvent TFE, and the continuous air flow within the fume hood. The drying times were set at nominally zero (the membranes were immersed as quickly as possible), 30 seconds, two minutes and eleven minutes of drying time. The eleven-minute time span was selected as the time after which the membrane surface took on a visually matte appearance indicating that the surface (and likely the entire micron-thick membrane) was free of unbound solvent. The same drying times were tested on a set of membranes which had no additives to account for the drying process on the overall formation of the membrane selective layer. Membranes cast with both low and high concentrations of B12 were also dried to find if the combination of small molecule additives and drying time had a synergistic effect in changing membrane selectivity.

In all combinations of additive concentration and drying time, there was no noticeable effect on the morphology of the membranes created. Representative SEM micrographs for each combination can be seen in the appendix. It was also found that there was no significant trend in initial water permeance with changes in the air drying time. Figure 31 shows that there is a much greater effect on water permeance from additive content than from air drying time.

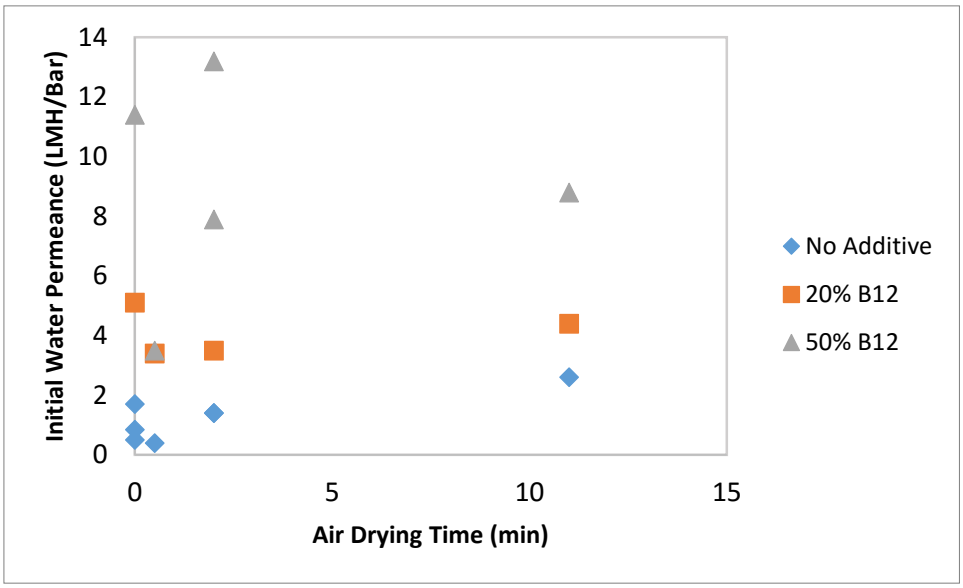

Figure 31: Water permeance as a function of air drying time before immersion in IPA and the concentration of Vitamin B12 in the casting solution.

Figure 32 shows the rejection curves constructed for each combination of additive concentration and drying time. No statistically relevant difference was observed when the drying time was changed. While there is some variation in the rejection of Vitamin B12, the trends are not monotonic. Furthermore, rejections in the 20-80% range such as those recorded for the imprinted membranes tend to have larger variabilities.

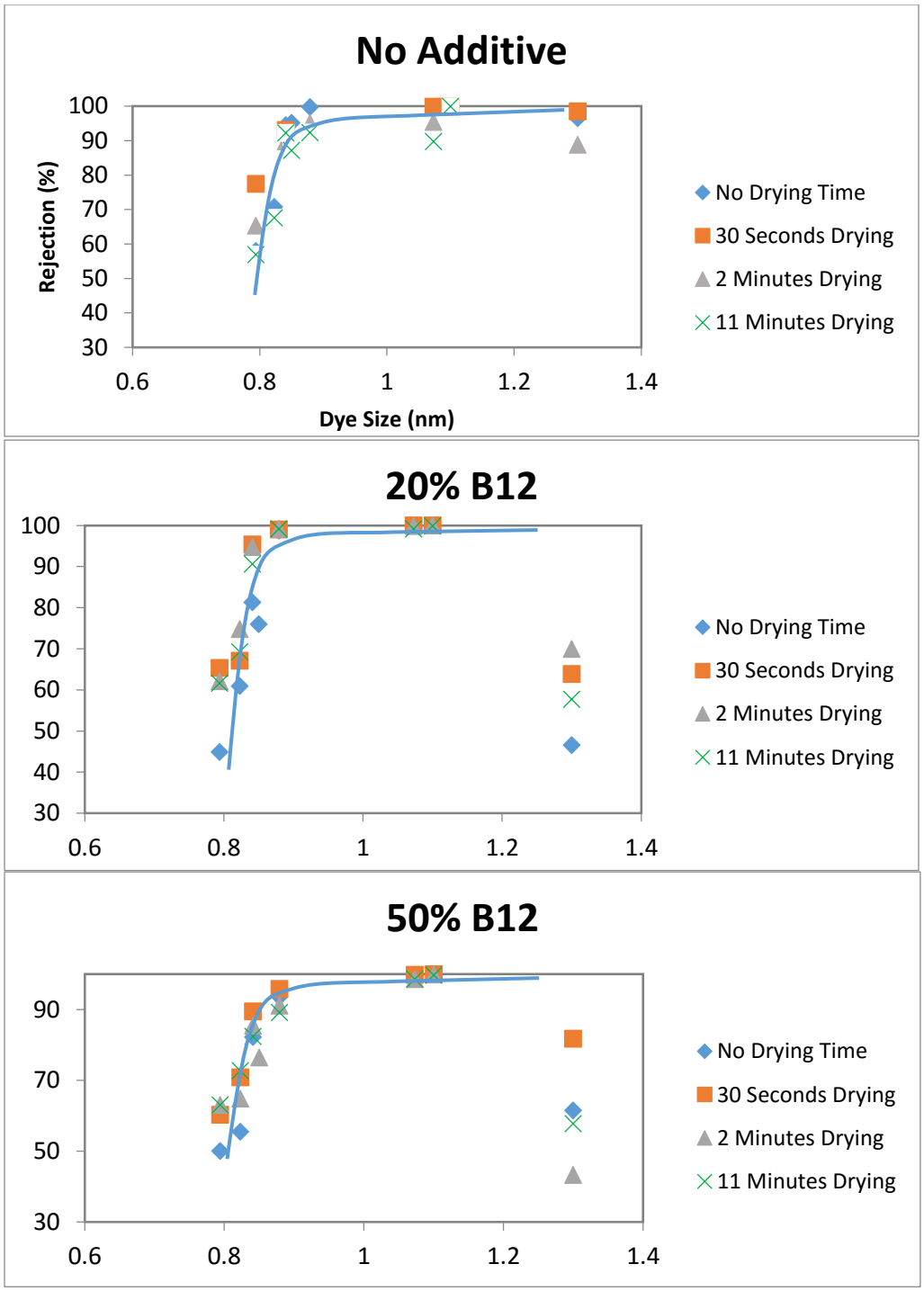

Figure 32: Effect of air drying time on the size-based selectivity of membranes cast without additive, as well as 20% and 50% Vitamin B12.

Thus, these results indicate that changing the drying time does not significantly affect the success of molecular imprinting for membranes prepared with Vitamin B12 as an additive. This is likely due to the fact that Vitamin B12 is not very soluble in IPA. A large

portion of the Vitamin B12 remains in the selective layer even after the membrane is immersed into this bath as exhibited by the bright pink coloring of the selective layer. Vitamin B12 is removed effectively after immersion into water. Thus, the additive has a long residence time even without a drying step. Figure 33 shows that after the 20 minute IPA bath, the cast membranes retain most of their Vitamin B12 content, leaving the coagulation bath unaltered in color. After the same period of time immersed in water, the Vitamin B12 has leached significantly and has turned the non-solvent bath pink. Overall, it usually takes about 60 to 80 minutes for the Vitamin B12 to mostly leave the membrane, as established by the visibly white color of the polymer in the water bath.

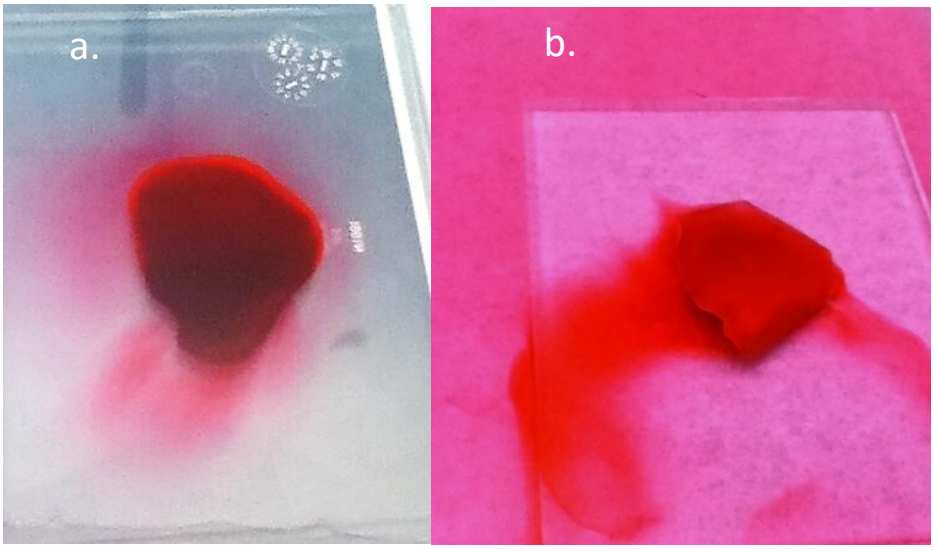

Figure 33: Photograph of a cast Vitamin B12-containing membrane a. after 20 minutes of immersion in IPA, and b. after subsequent immersion in water for 20 minutes.

Besides membrane selectivity, a change in drying time can also affect the morphology of the copolymer coating. At the end of the drying time, the overall composition of the copolymer solution will have shifted. This can lead to changes in the porosity of the selective layer that forms upon immersion into a non-solvent bath [1], [33]. The longer time period before immersing the membrane into the non-solvent bath

can also allow the penetration of the copolymer solution into the internal pores of the membrane due to capillary forces, negatively affecting membrane flux without corresponding gains in selectivity. To determine how the drying time affects the morphology of the selective layer, the membranes manufactured with various air drying times were imaged by scanning electron microscopy (Phenom G2 Pure Tabletop Scanning electron microscope (SEM) operating at 5 kV). Representative micrographs are shown for each Vitamin B12 concentration and drying time combination in Figure 34.

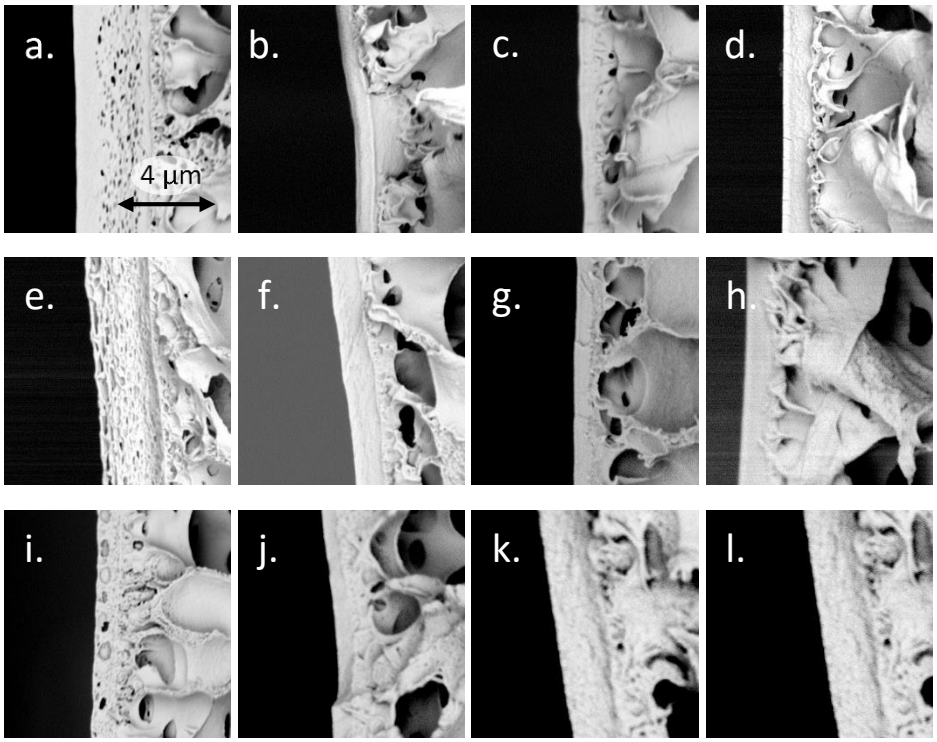

Figure 34: SEM micrographs of membrane selective layers produced with various Vitamin B12 concentrations and drying times. Images a. through d. are membranes cast with no Vitamin B12. e. through h. were cast with 20% Vitamin B12. i. through l. were cast with 50% Vitamin B12. The first column of membranes was cast with no drying time, the second column of membranes was cast with 30 seconds of drying time, the third column of membranes was cast with 2 minutes of drying time, and the last column of membranes was cast with 11 minutes of drying time.

The thickness of the selective layer was measured for each membrane to determine if there were any significant changes with drying time. Figure 35 shows that, for all Vitamin B12 concentrations, as drying time increases, the thickness of the coated

polymer membrane tends to become more uniform and typically of a smaller size. Each datum in this figure was collected from a different coated sheet of membrane. It is important to note that these thickness data points were generated from images taken on membrane samples which were cut from sections of the coated sheet that were as close to the tested swatch as possible. These results appear to be in contrast to the assertion made by Aroon that a longer evaporation time should yield a thicker membrane, whereas a shorter period leads to a thinner solidified coating which can display different separation properties from the thicker counterpart [36].

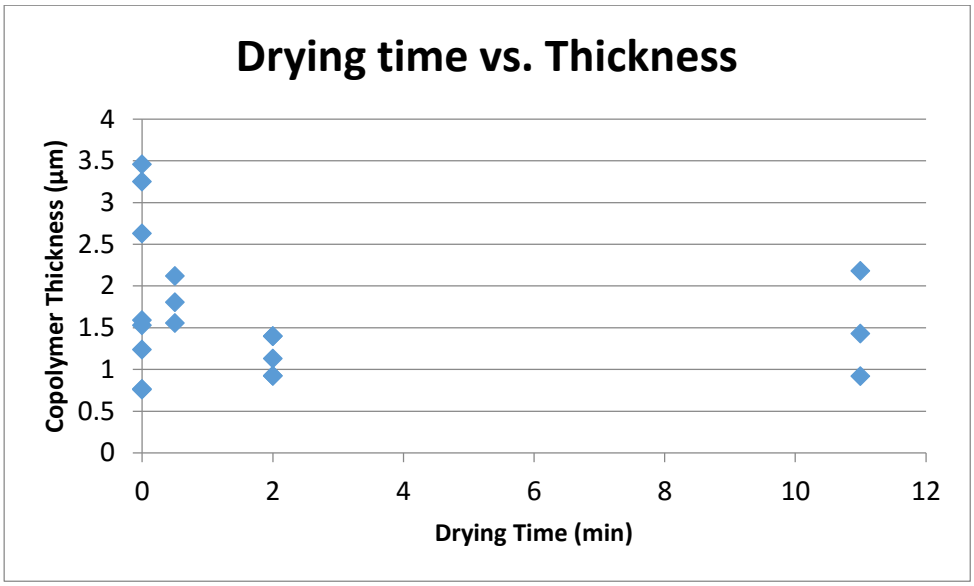

Figure 35: Coated polymer thickness varying with air drying time for the neat polymer, 20% and 50% B12 additive.

3.4 Effect of Excluding Immersion in an Isopropyl Alcohol Non-Solvent Bath

It has been established that the speed with which a polymer is solidified in a coagulation bath can have a profound effect on the final form of that polymer [33]. Depending on the speed of mass transfer of non-solvent into the polymer-solvent solution (which is in part a function of the depth of quench into the single phase region) we can observe greatly varying morphologies and interactions between the polymer and

its surroundings. To this end, we investigated the effect of an alternative coagulation approach to incorporate into the membrane manufacturing process. The previously described membrane manufacturing method was altered so that the coated membrane solution was first dried, and then transferred directly to the water bath without being first immersed in isopropyl alcohol. This modification can also lead to a simpler and cheaper membrane manufacturing process by removing the need for an additional non-solvent bath, filled with a flammable organic liquid.

When membranes were transferred directly to water after drying, a change was observed in the diffusion of the Vitamin B12 additive. In this manufacturing run, it was observed that the B12 remained in the polymer film for a discernable amount of time before diffusing into the water. As discussed, B12 was selected in part because it is highly soluble in water, lending to its ability to wash out of the polymer structure when the polymer is immersed in water for freezing. Vitamin B12 has a visible pink color in water, and we were able to observe this color transition from the surface of the membrane to the water bath. There was a small amount of B12 which was observed to immediately leach from the membrane, however, B12 continued to separate from the membrane continuously over the first 30 minutes of immersion in water. Since the object of adding B12 (and other additives) to the casting solution is to affect the physical behavior of the polymer zwitterion chains and glassy walls, this could imply that the elimination of an IPA wash step could have the immediate effect of decreasing the time of retention of an additive. It is possible that this residence time allows the walls of the polymer to freeze in place while additive molecules are present, but that the additive will be freed soon after it has served its intended purpose. In this case, the time over which the additive and

polymer chains have to interact would be an important factor in determining the degree to which imprinting could take place in the material.

Figure 36 shows the results of a battery of filtration tests performed on membranes cast without an IPA wash step from casting solutions containing no additive, 50 wt% PPS and 50 wt% Vitamin B12. Unfortunately, only one filtration datum was able to be collected for each dye in each formulation. Based on this limited data set, it appears that elimination of the IPA wash step may hamper the imprinting effect as interpreted by the location of the Vitamin B12 rejection data at a diameter of 1.3 nm. It can be said that as with the alterations to additive content when an IPA step was used, this change to the casting procedure does not change the location of the size-based cut-off.

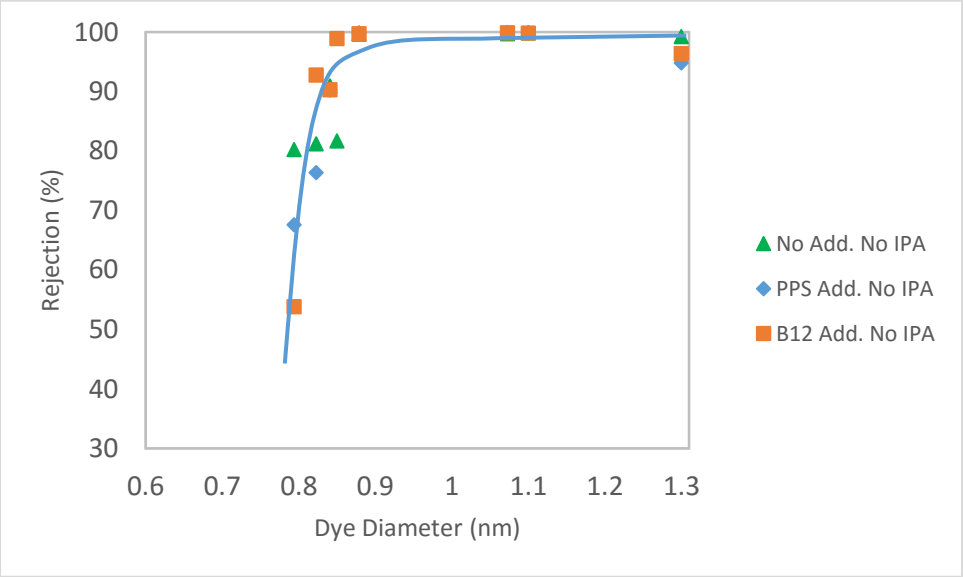

Figure 36: Effect of additive molecules upon dye retention for membranes cast without an IPA wash step.

3.5 Understanding Molecular Imprinting in Zwitterionic Membranes

To perform a holistic analysis of the molecular imprinting effect in membranes with P40 copolymer selective layers prepared with various additives, we directly compared how the rejection of the additive (i.e. imprinted molecule) and another solute

of similar size but different chemical structure changed. We focused these studies on Vitamin B12, the zwitterionic molecules used in most of the studies here, and Direct Red 80, an anionic dye of similar size. In addition to these two solutes, we studied how PPS and SBMA would perform as additives that are similar but not identical to Vitamin B12 due to their zwitterionic structure and strong dipole moment capable of interacting with the SBMA groups in the nanochannels. We have established that the inclusion of additive molecules to the casting solution does not affect the channel size, so the inclusion of rejection data for small solutes here is no longer necessary.

Figure 37: Rejection of Vitamin B12 solute in membranes cast with various additive concentrations.

Figure 37 shows the rejection of Vitamin B12 by the various membranes created for this study. The most significant molecular imprinting effect is observed for the case where Vitamin B12 is used as both the polymer solution additive and the filtration solution solute. It can be seen that the addition of 20% Vitamin B12 by mass to the membrane allows for Vitamin B12 to be rejected over 30 percentage points lower when compared to membranes made from additive-free polymer. When the casting solution

composition contained 50% Vitamin B12 by weight, we see a similar Vitamin B12 rejection indicating the further addition of Vitamin B12 does not further change the selectivity.

The same effect is seen to a lesser degree when the SBMA monomer is used as the additive in the membranes. In these cases, the rejection of zwitterionic Vitamin B12 is lower than in the virgin membranes, but the drop is significantly less pronounced than when the same molecule is used as an imprinting agent and filtration solute.

The next step toward investigating the molecular imprinting mechanism was to decipher if this change in filtration performance is an effect of the size of the Vitamin B12 molecule, or the structure. It seems likely that the zwitterion pendant groups in the P40 membrane would be prime sites for imprinting interactions based on electronic structure, so we next manufactured membranes with another small molecule zwitterion that is much smaller than the Vitamin B12 structure (PPS), as well as an additive which is roughly the same size as Vitamin B12 but is not zwitterionic (Direct Red 80). The results of Vitamin B12 rejection experiments with these casting solution additives (Figure 37) show that the addition of zwitterionic additives yield performance decreases in Vitamin B12 rejection, even when the additive is of a very different size compared to the filtrate. That is to say, when the zwitterion PPS was used as the additive in the casting solution, we observe a drop in the rejection of Vitamin B12 solutions. Because the PPS molecule is similar to Vitamin B12 in its zwitterionic nature that leads to a very high dipole moment but very different from B12 in size and physical shape, the drop in rejection of B12 is only about 20 percentage points at the highest additive loading. This decrease in rejection was much more prominent when Vitamin B12 was used as both the casting additive and solute.

In contrast, membranes prepared with Direct Red 80 as an additive show no change in Vitamin B12 rejection despite the size similarity between the two molecules. These results inform us that the drop in rejection of Vitamin B12 solutions is the result not simply of the presence of an additive, or simply the presence of an additive of a specific size, but of interactions which are dependent upon size and charge distribution.

After these studies, we aimed to determine if this molecular imprinting effect was specific to zwitterionic solutes, or if similar changes in selectivity can be achieved using other additives. To this end, the rejection of Direct Red 80, an anionic dye roughly the same size as Vitamin B12, was measured for the same set of membranes (Figure 38).

Figure 38: Rejection of Direct Red 80 in membranes cast with various guest molecule concentrations.

There was no measurable change in the rejection of Direct Red 80 with the use of any of these additives. This tells us that the molecular imprinting effect was not observed with Direct Red 80, implying this capability may be limited to zwitterionic solutes. While

zwitterion additives can be used to change the way zwitterion solutes are filtered through P40 membranes, the addition of additives to the casting solution has no effect upon non-zwitterionic solutes. Furthermore, non-zwitterionic additives do not significantly alter the selectivity of these membranes, at least for the limited range of compounds tested in this study. These results lead to the tentative conclusion that molecular imprinting has been achieved wherein interactions between the SBMA pendant groups and zwitterion additive molecules is capable of affecting filtration characteristics of this material.

The likely explanation for this observation results from the geometry and placement of charges in zwitterionic and ion molecules. In P40, the charges are always approximately the same distance from each other, determined by the alkyl spacer between the charged groups. When a similarly shaped zwitterion small molecule is introduced to the system, the positive segment of the SBMA polymer zwitterion can associate favorably with the negative moiety of the additive zwitterion and vice versa. These interactions are displayed schematically on the left side of Figure 39. It would appear that when the target molecule is a zwitterion of different geometry from the solute filtered, the complementary interactions still occur, and positive charges are always able to associate with negative charges, but because of the shape of the imprinted sites, there is increased distance between oppositely charged species when solutes are introduced, leading to reduced specificity. However, in the case where a charged target molecule such as Direct Red 80 is added to the casting solution, one of the target's negative sulfonate groups can associate favorably with the positively charged section of the polymer zwitterion, but in doing so it will necessarily orient another of its negatively charged groups with the zwitterion's negative moiety, creating an unfavorable

electrostatic interaction. This repulsion, it would appear, greatly hinders the ability of the zwitterion in the membrane to orient itself complementarily to the target molecule.

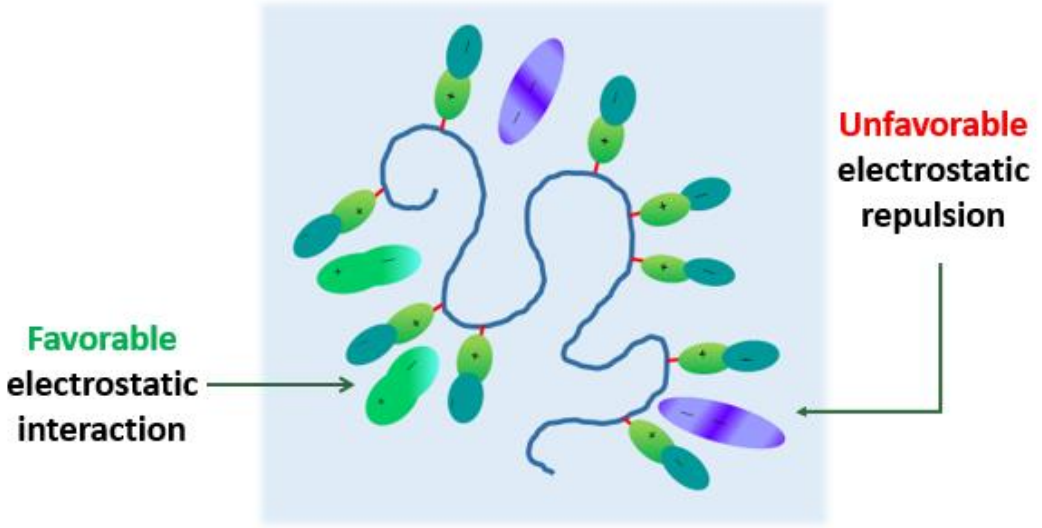

Figure 39: Schematic of favorable zwitterion-zwitterion interactions (left) and slightly unfavorable zwitterion-ion interactions (right).

While the limited amount of data presented here support this proposed hypothesis, the results presented here are valid only for the zwitterion membrane material and target molecules used here. If a general understanding of these interactions is desired, there must be extensive study into the other various interactions which could be taking place, as well as to the various aspects of the membrane casting process which could be playing a role in the ultimate filtration behavior of the material.

4 Conclusions and Future Directions

The work presented here contains experiments conducted in attempts to alter the filtration capabilities of thin film composite membranes cast from the PTFEMA-*r*-SBMA zwitterionomer. Previous studies in the Asatekin lab have shown that this material self-assembles into thin films that serve as selective layers for membranes with size-based

filtration cutoff at around 1nm. The alteration of this property was the primary objective of this work. Numerous attempts were made to change the size of the channels formed in the membrane selective layer and ultimately the size-based filtration capabilities of the material were found to be robust. Molecular imprinting was established as a viable selectivity customization option. It was possible to purposefully create membranes which allow passage of zwitterion solutes which would ordinarily be too large to pass through the membrane barrier.

In a first attempt to alter the selectivity of the polymer film, the casting procedure was modified to include time after the initial casting before the polymer was immersed in isopropyl alcohol. This change was intended to slow the hardening of the polymer solution into its final morphology. Drying was allowed to proceed for short time periods, and for long enough for the solvent to visibly leave the solution. In all cases, the selectivity of the membrane created was unchanged from what was observed in initial studies with unmodified procedures. As in previous filtration tests, dye solutes were rejected based only on the basis of size, and the cutoff was at the same point, approximately 1 nm.

The complete removal of the IPA wash step was also investigated as a means to change the selectivity of the membranes, with similar results. In all cases, it appears the speed at which the polymer solution composition exits the solubility range does not play a significant part in the size of the periodic structures resulting from the self-assembly of the zwitterionic polymer chain. With this in mind, any future efforts into industrialization of this material as a filtration medium should consider altering the manufacturing technique to exclude this extraneous step. No change in rejection capabilities was observed upon addition or exclusion of the IPA step, and the incorporation of IPA into a

large-scale manufacturing operation is inherently expensive and dangerous because of IPA's volatility and flammability.

To elucidate an understanding of the way small molecule additives to the casting solution might interact with the various microphases in the copolymer material, tests were conducted with Nile Red, a molecule whose absorbance spectrum is changed by the environment in which it resides. Tests were conducted to establish if the absorbance of Nile Red in the copolymer was more similar to either of the homopolymers whose monomers it contains. It was found that the absorbance of Nile Red in the copolymer is more closely related to the absorbance in the zwitterionic SBMA than the hydrophobic TFEMA. This lead to the conclusion that in the case of Nile Red as a small molecule additive, the additive segregates into the zwitterion phase more than the hydrophobic phase. While this cannot give concrete information on the segregation of the other additives used, it does offer analogous information on how a similar structure interacts with the copolymer phases, allowing a more refined understanding of the underlying reasons for the observations made with additives such as Vitamin B12 and Direct Red 80.

Tests were conducted with additives to more fully characterize the interactions which could be imposed in the system. Some of the additives to the casting solution were zwitterions, such as Vitamin B12, Pyridinio Propane Sulphonate, and Sulfobetaine Methacrylate, while others were simply charged, such as Direct Red 80. These tests showed that in all cases, the additive cannot effect the size of the channels in the selective layer, but they can create favorable interaction sites under the right circumstances. When Vitamin B12 was added to the casting solution, the rejection of the large Vitamin B12 molecule dropped significantly below what would be expected simply based on size. This effect was also seen for Vitamin B12 solute when zwitterionic Pyridinio Propane

Sulphonate was added, but the effect was not observed for similarly large but non-zwitterionic Direct Red 80. This leads to the conclusion that the addition of zwitterionic small molecules to the casting solution could create molecularly imprinted sites with memory for the solutes which would be present as feed solutions, and that this causes a change in the filtration capability of the membrane based on manufacturing techniques.

It appears that the larger Vitamin B12 molecule was more capable of creating imprinted sites with recognition for Vitamin B12 solutes as compared to PPS. On the other hand, the incorporation of PPS into the casting solution appears to have had a much bigger effect on the glass transition behavior of the copolymer. From this, we may conclude that an additive's shape similarity to a target feed is a more important factor when designing for separation ability, and size is a more important factor when attempting to increase polymer chain motion and effect plasticization effects.

To date, molecular imprinting has been primarily applied to adsorptive separations, and it is often only possible to incorporate the effect during the synthesis of the polymeric material itself. The ability to impose such a change at the manufacturing stage of the membrane's life, as opposed to the synthesis phase is a significant development in the understanding of this material, and in the ways molecular imprinting can be used in filtration situations.

To aid in the understanding of the copolymer material and to create a more fine-tuned manufacturing sequence, we offer some recommendations for future investigators of this type of material. We first recommend an investigation into the effects of casting parameters beyond the exclusion of the IPA step and the inclusion of casting solution additives. Hoek describes how the addition of solvent into the non-solvent bath can

change the time the polymer film takes to precipitate and that adding a small amount can greatly increase the flux of the resulting membrane [9]. This relies on the concept of quench depth into the two-phase region of the ternary phase diagram. When a solution moves from the soluble region of the diagram to the phase-separation region, the distance into that region and the rate at which it does so can have a profound influence on the morphology of the precipitated material's morphology. By investigating in this vein, we could gain an understanding of the morphological changes future investigators could impose on their membrane films by simply changing the composition of the non-solvent bath.

It has also been suggested that changing the temperature of the coagulating bath can change the size of macrovoids in the polymer layer as well as selective layer thickness, pore size and permeability [9], [33], [56]. This effect may be enhanced when the polymer solution also contains small molecule additives [9]. As such, the temperature of the non-solvent into which the polymer layer is immersed poses an interesting additional parameter which could be investigated to further characterize the behavior of this polymer-solvent-non-solvent system.

It is conceivable that the effects of molecular imprinting could be undone at high temperatures, such as above the glass transition temperature of the hydrophobic component of our polymer material. If the material is brought above some critical temperature, it is conceivable that the pendants would become free to move from their imprinted configuration into another thermodynamically favorable stance. Such annealing would serve to essentially "turn off" the special selectivity achieved by imprinting and may provide an avenue to change the filtration characteristics of an imprinted membrane after it has been manufactured. While this would likely be a change

that could not be undone in the polymer morphology, it has potential applications in serial filtrations, and we would, therefore, suggest this as an avenue of future investigation. It is also an interesting alternative approach to verify that a molecular imprinting process is in effect in this system.

Because the main conclusion of this work is that molecular imprinting can be used to alter the rejection of large zwitterion solutes when similarly shaped zwitterions are incorporated into the casting solution, it should be investigated whether this can be extended to anionic solutes as well. It has been hypothesized here that favorable interactions between zwitterion additives and zwitterionic polymer pendant groups create the environment necessary for imprinting to take place. It may be the case that an analogous material could be made using anionic polymer pendant groups which could interact similarly with cationic additives such as Alcian Blue or Brilliant Green. In that case, we might expect to see imprinting when a dye such as Direct Red 80 is incorporated in the casting solution, but not see such an effect when Vitamin B12 is added. This type of study would provide deeper insight into the interactions which are taking place between additives and polymers. A potential challenge would be the removal of the imprinting molecule from the polymer, and the strength of its adsorption during filtration.

When molecules are transported through channels, they can sometimes be transiently trapped by selective sites along the channel [59]. These trapping events occur reversibly and last only for relatively short timespans. In this situation of “facilitated diffusion,” molecular dynamics studies have shown that the transport of individual molecules can be enhanced. As one might expect, when a low-affinity molecule is passed through the channels, there is no preferential binding, and the transport is not enhanced. However, in the case where selective and non-selective molecules are introduced

together, it is found that the lower affinity species enhances the transport of the higher affinity species. Because of this theoretical result, an interesting experiment would be to introduce Vitamin B12 (which has a high affinity for the molecularly imprinted pore walls) and Direct Red 80 or PPS (with a low affinity) in a single feed solution. Under such conditions, we may find that the rejection of Vitamin B12 can be made to drop even lower than we have observed in experiments which only use Vitamin B12 solutions. Because the defining feature of this work is the ability to lower the rejection of molecules like Vitamin B12 by imposing imprinting, the ability to enhance this effect by simply adding another molecule to the feed solution could be a powerful tool, especially in the case where the added solute is fully rejected itself, as in the case of Direct Red 80.

Appendix A: Sample NMR monomer ratio calculation

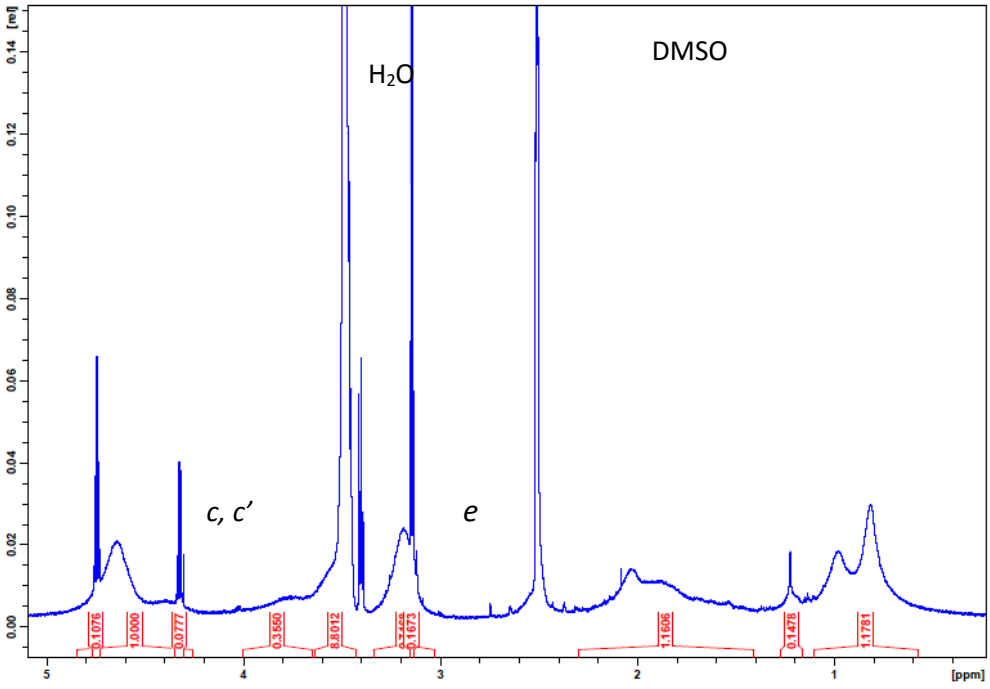

Figure A 1: Proton NMR spectrum of P40 material after non-solvent wash.

Because peak *e* represents the combined intensity from the six protons in the methyl groups of the SBMA quaternary amine structure,

$$0.72 = 6 * SBMA$$

$$\therefore SBMA = 0.12$$

The sum of the intensities of peak *c* and *c'* represents the combined signals from two equivalent protons in both the SBMA and TFEMA monomers. To see this intensity, it is necessary to subtract the intensities that result from the residual solvent in the polymer sample.

$$1.00 - 0.11 - 0.08 = 2(SBMA + TFEMA)$$

$$0.405 = TFEMA + 0.12$$

$$\therefore 0.285 = TFEMA$$

The mole fraction of each monomer in the polymer will be the signal present from that monomer as a fraction of the total signal resulting from both monomers.

$$Mol\%\ SBMA = \frac{SBMA}{SBMA + TFEMA} * 100\%$$

$$Mol\%\ SBMA = \frac{0.12}{0.12 + 0.285} * 100\%$$

$$\therefore Mol\%\ SBMA = 29.6\%$$

$$Mol\%\ TFEMA = \frac{TFEMA}{SBMA + TFEMA} * 100\%$$

$$Mol\%\ SBMA = \frac{0.285}{0.12 + 0.285} * 100\%$$

$$\therefore Mol\%\ SBMA = 70.4\%$$

Now the molar mass of each monomer can be used to convert the mole fraction to a mass fraction. The molar mass of SBMA is 279.35 Da and the molar mass of TFEMA is 168.11 Da. For this calculation, a basis of 1 mole of monomer was selected, allowing the mole fractions of each monomer to be easily converted into a definite molar quantity of monomer.

$$0.296\ mol\ SBMA * 279.35\ \frac{g\ SBMA}{mol\ SBMA} = 82.68g\ SBMA$$

$$0.704\ mol\ TFEMA * 168.11\ \frac{g\ TFEMA}{mol\ SBMA} = 118.35g\ TFEMA$$

$$weight\%\ SBMA = \frac{82.68g}{82.68g + 118.35g} * 100\% = 41.1\%$$

$$weight\%\ TFEMA = \frac{118.35g}{82.68g + 118.35g} * 100\% = 58.9\%$$

Appendix B: SEM Micrographs of Membranes made with Various Additives

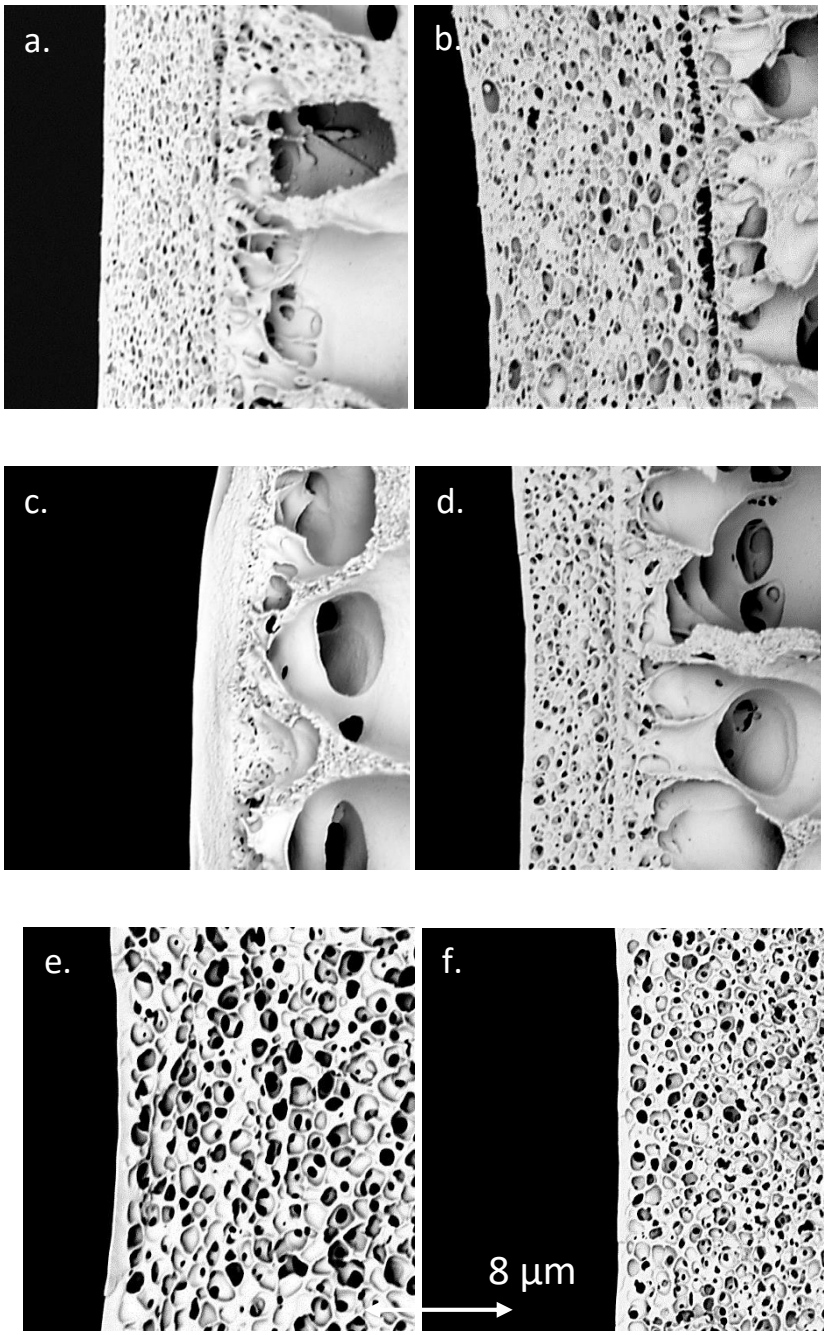

Figure A 2: Micrographs of membranes cast with a. 20% Direct Red 80, b. 50% Direct Red 80, c. 20% PPS, d. 50% PPS, e. 20% SBMA, f. 50% SBMA, each cast with a 20-minute immersion in IPA before final solidification.

Bibliography

[1] R. W. Baker, *Membrane Technology and Applications*, 3rd ed. Chichester: John Wiley and Sons, 2012.

[2] L. Chen, S. Xu, and J. Li, "Recent advances in molecular imprinting technology: current status, challenges and highlighted applications," *Chem. Soc. Rev.*, vol. 40, no. 5, p. 2922, 2011.

[3] P. Bengani, Y. Kou, and A. Asatekin, "Zwitterionic copolymer self-assembly for fouling resistant, high flux membranes with size-based small molecule selectivity," *J. Memb. Sci.*, vol. 493, pp. 755–765, 2015.

[4] N. M. Bergmann and N. A. Peppas, "Molecularly imprinted polymers with specific recognition for macromolecules and proteins," *Prog. Polym. Sci.*, vol. 33, no. 3, pp. 271–288, 2008.

[5] B. Gao, J. Wang, F. An, and Q. Liu, "Molecular imprinted material prepared by novel surface imprinting technique for selective adsorption of pirimicarb," *Polymer (Guildf).*, vol. 49, no. 5, pp. 1230–1238, 2008.

[6] V. P. Joshi, M. G. Kulkarni, and R. A. Mashelkar, "Enhancing adsorptive separations by molecularly imprinted polymers: Role of imprinting techniques and system parameters," *Chem. Eng. Sci.*, vol. 55, no. 9, pp. 1509–1522, 2000.

[7] B. Sellergren and T. Greibrook, "Molecular imprinting in separation science.," *J. Sep. Sci.*, vol. 39, pp. 38–40, 2016.

[8] B. Sellergren and T. Greibrook, "Molecular imprinting in separation

science.,” *J. Sep. Sci.*, vol. 32, pp. 3263–3264, 2009.

[9] G. R. Guillen, Y. Pan, M. Li, and E. M. V Hoek, “Preparation and characterization of membranes formed by nonsolvent induced phase separation: A review,” *Ind. Eng. Chem. Res.*, vol. 50, no. 7, pp. 3798–3817, 2011.

[10] M. Ulbricht, “Membrane separations using molecularly imprinted polymers,” *J. Chromatogr. B Anal. Technol. Biomed. Life Sci.*, vol. 804, no. 1, pp. 113–125, 2004.

[11] American Water Works Association, “Microfiltration and Ultrafiltration Membranes for Drinking Water,” vol. 0, no. December, p. 257, 2011.

[12] K. Sutherland, *Profile of the International Membrane Industry*, 3rd ed., no. October 2003. Oxford: Elsevier Science Ltd, 2003.

[13] A. Asatekin and C. Vannucci, “Self-Assembled Polymer Nanostructures for Liquid Filtration Membranes: A Review,” *Nanosci. Nanotechnol. Lett.*, vol. 7, pp. 21–32, 2015.

[14] W. M. Deen, “Hindered Transport of Large Molecules in Liquid-Filled Pores,” *AIChE J.*, vol. 33, no. 9, pp. 1409–1425, 1987.

[15] K. S. Spiegler and O. Kedem, “Thermodynamics of hyperfiltration (reverse osmosis): criteria for efficient membranes,” *Desalination*, vol. 1, no. 4, pp. 311–326, 1966.

[16] W. R. Bowen and J. S. Welfoot, “Modelling the performance of membrane nanofiltration-critical assessment and model development,” *Chem. Eng.*

Sci., vol. 57, no. 7, pp. 1121–1137, 2002.

[17] A. Szymczyk and P. Fievet, “Investigating transport properties of nanofiltration membranes by means of a steric, electric and dielectric exclusion model,” *J. Memb. Sci.*, vol. 252, no. 1–2, pp. 77–88, 2005.

[18] A. Asatekin and A. M. Mayes, “Polymer filtration membranes,” in *Encyclopedia of Polymer Science and Technology*, no. 1, New York: John Wiley and Sons, 2009.

[19] W. A. P. Yizhou Zhang, Jessica L. Sargent, Bryan W. Boudouris, “Nanoporous membranes generated from self-assembled block polymer precursors: Quo Vadis?,” *J. Appl. Polym. Sci.*, vol. 132, no. 21, p. 41683, 2015.

[20] M. F. a. Goosen, S. S. Sablani, H. Al-Hinai, S. Al-Obeidani, R. Al-Belushi, D. Jackson, H. Al-Hinai, S. Al-Obeidani, R. Al-Belushi, and D. Jackson, “Fouling of Reverse Osmosis and Ultrafiltration Membranes: A Critical Review,” *Sep. Sci. Technol.*, vol. 39, no. 10, pp. 2261–2297, 2005.

[21] W. Guo, H. H. Ngo, and J. Li, “A mini-review on membrane fouling,” *Bioresour. Technol.*, vol. 122, pp. 27–34, 2012.

[22] K. J. Hwang and C. L. Hsueh, “Dynamic analysis of cake properties in microfiltration of soft colloids,” *J. Memb. Sci.*, vol. 214, no. 2, pp. 259–273, 2003.

[23] S. Bhattacharjee, J. C. Chen, and M. Elimelech, “Coupled model of concentration polarization and pore transport in crossflow nanofiltration,”

Am. Inst. Chem. Eng. AIChE J., vol. 47, no. 12, pp. 2733–2746, 2001.

[24] H. Du and X. Qian, "The hydration properties of carboxybetaine zwitterion brushes," *J. Comput. Chem.*, pp. 877–885, 2016.

[25] J. B. Schlenoff, "Zwitteration: Coating surfaces with zwitterionic functionality to reduce nonspecific adsorption," *Langmuir*, vol. 30, no. 32, pp. 9625–9636, 2014.

[26] C. M. Case, *Physical Principles of Flow in Unsaturated Porous Media*. New York: Oxford University Press, 1994.

[27] C. Nurra, L. Pitol-Filho, R. Curraud, S. Pertuz, D. Puig, M. A. Garcia, J. Salvado, and C. Torras, "Toward the Prediction of Porous Membrane Permeability From Morphological Data," *Polym. Eng. Sci.*, vol. 56, no. 1, pp. 118–124, 2016.

[28] C. Vannucci, I. Taniguchi, and A. Asatekin, "Nanoconfinement and Chemical Structure Effects on Permeation Selectivity of Self-Assembling Graft Copolymers," *ACS Macro Lett.*, vol. 4, no. 9, pp. 872–878, 2015.

[29] S. Achanta, J. H. Cushman, and M. R. Okos, "On multicomponent, multiphase thermomechanics with interfaces," *Int. J. Eng. Sci.*, vol. 32, no. 11, pp. 1717–1738, 1994.

[30] L. M. Robeson, Z. P. Smith, B. D. Freeman, and D. R. Paul, "Contributions of diffusion and solubility selectivity to the upper bound analysis for glassy gas separation membranes," *J. Memb. Sci.*, vol. 453, pp. 71–83, 2014.

[31] G. M. Geise, B. D. Freeman, and D. R. Paul, "Sodium chloride diffusion in

sulfonated polymers for membrane applications," *J. Memb. Sci.*, vol. 427, pp. 186–196, 2013.

[32] S. Loeb and S. Sourirajan, "High flow porous membranes for separating water from saline solutions," US3133132 A, 1964.

[33] V. Abetz, "Isoporous Block Copolymer Membranes," *Macromol. Rapid Commun.*, vol. 36, pp. 10–22, 2015.

[34] K.-V. Peinemann, V. Abetz, and P. F. W. Simon, "Asymmetric superstructure formed in a block copolymer via phase separation," *Nat. Mater.*, vol. 6, no. 12, pp. 992–996, 2007.

[35] A. Akthakul, R. F. Salinaro, and A. M. Mayes, "Antifouling polymer membranes with subnanometer size selectivity," *Macromolecules*, vol. 37, no. 20, pp. 7663–7668, 2004.

[36] M. a. Aroon, a. F. Ismail, M. M. Montazer-Rahmati, and T. Matsuura, "Morphology and permeation properties of polysulfone membranes for gas separation: Effects of non-solvent additives and co-solvent," *Sep. Purif. Technol.*, vol. 72, no. 2, pp. 194–202, 2010.

[37] M. Sadrzadeh and S. Bhattacharjee, "Rational design of phase inversion membranes by tailoring thermodynamics and kinetics of casting solution using polymer additives," *J. Memb. Sci.*, vol. 441, pp. 31–44, 2013.

[38] P. G. Khalatur and A. R. Khokhlov, "Nonconventional scenarios of polymer self-assembly," *Soft Matter*, vol. 9, no. 46, pp. 10943–10954, 2013.

[39] A. Asatekin, S. Kang, M. Elimelech, and A. M. Mayes, "Anti-fouling

ultrafiltration membranes containing polyacrylonitrile-graft-poly(ethylene oxide) comb copolymer additives," *J. Memb. Sci.*, vol. 298, no. 1–2, pp. 136–146, Jul. 2007.

[40] A. Asatekin, E. A. Olivetti, and A. M. Mayes, "Fouling resistant, high flux nanofiltration membranes from polyacrylonitrile-graft-poly(ethylene oxide)," *J. Memb. Sci.*, vol. 332, no. 1–2, pp. 6–12, 2009.

[41] S. R. Wickramasinghe S. Ranil, E. D. Stump, D. L. Grzenia, S. M. Husson, and J. Pellegrino, "Understanding virus filtration membrane performance," *J. Memb. Sci.*, vol. 365, no. 1–2, pp. 160–169, 2010.

[42] S. Y. Yang, J. Park, J. Yoon, M. Ree, S. K. Jang, and J. K. Kim, "Virus filtration membranes prepared from nanoporous block copolymers with good dimensional stability under high pressures and excellent solvent resistance," *Adv. Funct. Mater.*, vol. 18, no. 9, pp. 1371–1377, 2008.

[43] T. Y. Liu, H. G. Yuan, Q. Li, Y. H. Tang, Q. Zhang, W. Qian, B. Van Der Bruggen, and X. Wang, "Ion-Responsive Channels of Zwitterion-Carbon Nanotube Membrane for Rapid Water Permeation and Ultrahigh Mono-/Multivalent Ion Selectivity," *ACS Nano*, vol. 9, no. 7, pp. 7488–7496, 2015.

[44] S. Park, D. H. Lee, J. Xu, B. Kim, S. W. Hong, U. Jeong, T. Xu, and T. P. Russell, "Macroscopic 10-terabit-per-square-inch arrays from block copolymers with lateral order.," *Science*, vol. 323, no. February, pp. 1030–1033, 2009.

[45] G. S. Georgiev, E. B. Kamenska, E. D. Vassileva, I. P. Kamenova, V. T.

Georgieva, S. B. Iliev, and I. A. Ivanov, “Self-Assembly , Antipolyelectrolyte Effect , and Nonbiofouling Properties of Polyzwitterions,” vol. 7, pp. 1329–1334, 2006.

[46] S. Bureekaew, S. Shimomura, and S. Kitagawa, “Chemistry and application of flexible porous coordination polymers,” *Sci. Technol. Adv. Mater.*, vol. 9, no. 1, p. 014108, 2008.

[47] K. B. Jirage, J. C. Hulteen, and C. R. Martin, “Effect of thiol chemisorption on the transport properties of gold nanotubule membranes,” *Anal. Chem.*, vol. 71, no. 21, pp. 4913–4918, 1999.

[48] S. H. Yoo, J. H. Kim, J. Y. Jho, J. Won, and Y. S. Kang, “Influence of the addition of PVP on the morphology of asymmetric polyimide phase inversion membranes: Effect of PVP molecular weight,” *J. Memb. Sci.*, vol. 236, no. 1–2, pp. 203–207, 2004.

[49] B. Chakrabarty, A. K. Ghoshal, and M. K. Purkait, “Preparation, characterization and performance studies of polysulfone membranes using PVP as an additive,” *J. Memb. Sci.*, vol. 315, no. 1–2, pp. 36–47, 2008.

[50] B. Jung, K. Y. Joon, B. Kim, and H. W. Rhee, “Effect of molecular weight of polymeric additives on formation, permeation properties and hypochlorite treatment of asymmetric polyacrylonitrile membranes,” *J. Memb. Sci.*, vol. 243, no. 1–2, pp. 45–57, 2004.

[51] H. Susanto and M. Ulbricht, “Characteristics, performance and stability of

polyethersulfone ultrafiltration membranes prepared by phase separation method using different macromolecular additives," *J. Memb. Sci.*, vol. 327, no. 1–2, pp. 125–135, 2009.

[52] N. Peng, T. S. Chung, and K. Y. Li, "The role of additives on dope rheology and membrane formation of defect-free Torlon® hollow fibers for gas separation," *J. Memb. Sci.*, vol. 343, pp. 62–72, 2009.

[53] Y. Mansourpanah and A. Gheshlaghi, "Effects of adding different ethanol amines during membrane preparation on the performance and morphology of nanoporous PES membranes," *J. Polym. Res.*, vol. 19, no. 12, 2012.

[54] B. Torrestiana-Sanchez, R. I. Ortiz-Basurto, and E. Brito-De La Fuente, "Effect of nonsolvents on properties of spinning solutions and polyethersulfone hollow fiber ultrafiltration membranes," *J. Memb. Sci.*, vol. 152, no. 1, pp. 19–28, 1999.

[55] J. M. P. Scofield, P. A. Gurr, J. Kim, Q. Fu, A. Halim, S. E. Kentish, and G. G. Qiao, "High-performance thin film composite membranes with well-defined poly(dimethylsiloxane)-b-poly(ethylene glycol) copolymer additives for CO2 separation," *J. Polym. Sci. Part A Polym. Chem.*, p. n/a–n/a, 2015.

[56] M. Wei, W. Sun, X. Shi, Z. Wang, and Y. Wang, "Homoporous Membranes with Tailored Pores by Soaking Block Copolymer/Homopolymer Blends in Selective Solvents: Dissolution versus Swelling," *Macromolecules*, 2015.

[57] L. Xu, C. Zhang, M. Rungta, W. Qiu, J. Liu, and W. J. Koros, “Formation of defect-free 6FDA-DAM asymmetric hollow fiber membranes for gas separations,” *J. Memb. Sci.*, vol. 459, pp. 223–232, 2014.

[58] C. Ayela, M. E. Benito-Pena, A. Biffis, M. Bompart, D. Carboni, P. J. Cywinski, G. Dvorakova, A. Falcimaigne-Cordin, K. Flavin, K. Haupt, G. Harvai, W. Kutner, A. V. Linares, G. J. Mohr, M. C. Moreno-Bondi, A. J. Moro, G. Orellana, M. Resmini, S. Suriyanarayanan, B. Tse Sum Bui, B. Toth, and J. L. Urraca, *Molecular Imprinting*. New York: Springer Heidelnberg, 2012.

[59] A. Zilman, S. di Talia, T. Jovanovic-Talisman, B. T. Chait, M. P. Rout, and M. O. Magnasco, “Enhancement of transport selectivity through nano-channels by non-specific competition,” *PLoS Comput. Biol.*, vol. 6, no. 6, pp. 1–11, 2010.

[60] V. Kochkodan, N. Hilal, V. Melnik, O. Kochkodan, and O. Vasilenko, “Selective recognition of organic pollutants in aqueous solutions with composite imprinted membranes,” *Adv. Colloid Interface Sci.*, vol. 159, no. 2, pp. 180–188, 2010.

[61] W. J. Cheong, S. H. Yang, and F. Ali, “Molecular imprinted polymers for separation science: A review of reviews,” *J. Sep. Sci.*, vol. 36, no. 3, pp. 609–628, 2013.

[62] K. Mosbach, “Molecular Imprinting,” *Trends Biochem. Sci.*, vol. 19, no. 1, pp. 9–14, 1994.

[63] S. A. Piletsky, E. V. Piletskaya, T. A. Sergeyeva, T. L. Panasyuk, and A. V. El'Skaya, "Molecularly imprinted self-assembled films with specificity to cholesterol," *Sensors Actuators, B Chem.*, vol. 60, no. 2, pp. 216–220, 1999.

[64] S. A. Piletsky, T. L. Panasyuk, E. V. Piletskaya, I. A. Nicholls, and M. Ulbricht, "Receptor and transport properties of imprinted polymer membranes - A review," *J. Memb. Sci.*, vol. 157, no. 2, pp. 263–278, 1999.

[65] G. a. Kryvshenko, P. Y. Apel, S. S. Abramchuk, and M. K. Beklemishev, "A Highly Permeable Membrane for Separation of Quercetin Obtained by Nickel(II) Ion-Mediated Molecular Imprinting," *Sep. Sci. Technol.*, vol. 47, no. August 2013, pp. 1715–1724, 2012.

[66] Q. Shao, Y. He, A. D. White, and S. Jiang, "Difference in hydration between carboxybetaine and sulfobetaine," *J. Phys. Chem. B*, vol. 114, no. 49, pp. 16625–16631, 2010.

[67] Q. Shao, Y. He, and S. Jiang, "Molecular dynamics simulation study of ion interactions with zwitterions.," *J. Phys. Chem. B*, vol. 115, no. 25, pp. 8358–8363, 2011.

[68] A. K. Dutta, K. Kamada, and K. Ohta, "Spectroscopic studies of nile red in organic solvents and polymers," *J. Photochem. Photobiol. A Chem.*, vol. 93, no. 1, pp. 57–64, 1996.

[69] H. Yanwen, A. M. Bardo, C. Martinez, and D. A. Higgins, "Characterization of Molecular Scale Environments in Polymer Films by Single Molecule

Spectroscopy," *J. Phys. Chem. B*, vol. 104, no. 2, pp. 212–219, 2000.

[70] G. Hungerford and J. A. Ferreira, "The effect of the nature of retained solvent on the fluorescence of Nile Red incorporated in sol-gel-derived matrices," *J. Lumin.*, vol. 93, no. 2, pp. 155–165, 2001.

[71] NIH, "Substance Name: Cyanocobalamin," 2015. [Online]. Available: http://chem.sis.nlm.nih.gov/chemidplus/rn/68-19-9. [Accessed: 17-Sep-2015].

[72] O. Ratcharak and A. Sane, "Surface coating with poly(trifluoroethyl methacrylate) through rapid expansion of supercritical CO2 solutions," *J. Supercrit. Fluids*, vol. 89, pp. 106–112, 2014.

[73] M. Galin, E. Marchal, A. Mathis, B. Meurer, Y. M. M. Soto, and J. C. Galin, "Poly(sulphopropylbetaines): 3. Bulk properties," *Polymer (Guildf).*, vol. 28, no. 11, pp. 1937–1944, 1987.

[74] B. Wunderlich, "Termination of crystallization or ordering of flexible, linear macromolecules," *J. Therm. Anal. Calorim.*, vol. 109, no. 3, pp. 1117–1132, 2012.